Atmos. Chem. Phys. Discuss., 13, 983–1044, 2013
www.atmos-chem-phys-discuss.net/13/983/2013/
doi:10.5194/acpd-13-983-2013

Atmospheric Chemistry and Physics Discussions

Kinetic regimes and limiting cases of gas uptake and heterogeneous reactions in atmospheric aerosols and clouds: a general classification scheme

T. Berkemeier[1,2,3], **A. J. Huisman**[2,*], **M. Ammann**[4], **M. Shiraiwa**[5], **T. Koop**[1], **and U. Pöschl**[3]

[1]Faculty of Chemistry, Bielefeld University, Bielefeld, Germany
[2]Institute for Atmospheric and Climate Science, ETH Zürich, Zürich, Switzerland
[3]Multiphase Chemistry Department, Max-Planck-Institute for Chemistry, Mainz, Germany
[4]Laboratory of Radiochemistry and Environmental Chemistry, Paul-Scherrer-Institute, Villigen, Switzerland
[5]Division of Chemistry and Chemical Engineering, California Institute of Technology, Pasadena, California, USA
[*]now at: Department of Chemistry, Union College, Schenectady, NY, USA

Received: 30 November 2012 – Accepted: 14 December 2012 – Published: 9 January 2013

Correspondence to: A. J. Huisman (huismana@union.edu)

Published by Copernicus Publications on behalf of the European Geosciences Union.

Abstract

Heterogeneous reactions are important to atmospheric chemistry and are therefore an area of intense research. In multiphase systems such as aerosols and clouds, chemical reactions are usually strongly coupled to a complex sequence of mass transport processes and results are often not easy to interpret.

Here we present a systematic classification scheme for gas uptake by aerosol or cloud particles which distinguishes two major regimes: a reaction-diffusion regime and a mass-transfer regime. Each of these regimes includes four distinct limiting cases, characterized by a dominant reaction location (surface or bulk) and a single rate-limiting process: chemical reaction, bulk diffusion, gas-phase diffusion or mass accommodation.

The conceptual framework enables efficient comparison of different studies and reaction systems, going beyond the scope of previous classification schemes by explicitly resolving interfacial transport processes and surface reactions limited by mass transfer from the gas phase. The use of kinetic multi-layer models instead of resistor model approaches increases the flexibility and enables a broader treatment of the subject, including cases which do not fit into the strict limiting cases typical of most resistor model formulations. The relative importance of different kinetic parameters such as diffusion, reaction rate and accommodation coefficients in this system is evaluated by a quantitative global sensitivity analysis. We outline the characteristic features of each limiting case and discuss the potential relevance of different regimes and limiting cases for various reaction systems. In particular, the classification scheme is applied to three different data sets for the benchmark system of oleic acid reacting with ozone. In light of these results, future directions of research needed to elucidate the multiphase chemical kinetics in this and other reaction systems are discussed.

ACPD
13, 983–1044, 2013

1 Introduction

Tropospheric aerosols are composed of organic and inorganic substances originating from direct emission of particles and from condensation of gas-phase species (Kanakidou et al., 2005). Aerosols are climate forcers (Streets et al., 2004; Yu et al., 2006; IPCC, 2007) and are implicated in human health effects (Bates, 1993; Jakab et al., 1995; McConnell et al., 2002; Nel, 2005) as well as other undesirable phenomena such as reduced visibility in urban and rural areas. At this time, the physical and chemical properties of aerosols are still poorly understood and despite extensive experimental and modeling efforts, many of the processes central to heterogeneous chemical processing of aerosols remain unclear (Kolb et al., 2010).

Most previous studies of the gas uptake into aerosol particles have used "resistor" models which account for physical and chemical processes for a single or at most a few physical domains within the aerosol particle by analogy to electrical circuits (an overview of resistor models in the canonical system of oleic acid – ozone heterogeneous reaction is given in Zahardis and Petrucci, 2007). Such models allow analytical expressions to be derived for uptake of trace gases or loss of condensed phase material in simplified, limiting cases. These analytical expressions can be used to calculate the underlying kinetic parameters such as reaction rate coefficients or the accommodation coefficient (which are applicable to a reaction system under any conditions) or the trace gas uptake coefficient γ (which is specific to the experimental conditions at which it was measured). Using this sort of framework has been fruitful in the past for a wide range of gas/particle processes, and was particularly successful in assessing key heterogeneous interactions of relevance to stratospheric ozone depletion (Hanson et al., 1994). Analysis based on limiting cases has found widespread acceptance and also forms the basis for the recent evaluations by the IUPAC Subcommittee for Gas Kinetic Data Evaluation (Crowley et al., 2010). Because a wide variety of processes are important to multiphase chemistry, it is less well understood than pure gas-phase

ACPD
13, 983–1044, 2013

chemistry (e.g. Abbatt et al., 2012) and new methods are needed to facilitate analysis and discussion.

Recently developed depth-resolved models for single particles or thin films that focus on chemistry, such as KM-SUB (Shiraiwa et al., 2010), and water diffusion, such as the ETH Diffusion Model (Zobrist et al., 2011), allow a more complete consideration of the time- and depth-resolved chemical and physical behavior of aerosol particles, leading to a better understanding of these reaction systems. Shiraiwa et al. (2011a) have shown that resistor models are not sufficient for systems in which the bulk material is radially inhomogeneous in concentration owing to, e.g. diffusion limitations.

Due to the complexity of numerical models such as these, it is often unclear which process is most important to model outputs. Sensitivity analysis provides a simple means of identifying the model parameters which most strongly influence the results (and thus are related to the rate-limiting process). Although many previous studies have employed a local approach, advanced computational tools exist to systematically calculate sensitivity coefficients and take into account higher order parameter effects (the "global methods" in Saltelli et al., 2008). As reviewed in Cariboni et al. (2007), global sensitivity methods have been applied to fields such as ecological modeling, and in atmospheric science advanced sensitivity methods have been applied to models of single gas-phase chemical reactions (e.g. Dunker, 1984) and regional ozone formation (Martien and Harley, 2006). However, to the authors' knowledge this type of sensitivity analysis has not been applied previously to a depth-resolved or resistor-style model of the physicochemical behavior of single aerosol particles.

Kinetic regimes and limiting cases allow classification of system behavior for analysis and comparison of model outputs with experimental results. In this work, we propose an enhanced set of limiting cases which can be used for conceptual discussion and analysis along with a systematic, numerically-based method for assigning a limiting case to a reaction system. This classification is compared with the outcome of a global sensitivity analysis to ensure that the system behavior is consistent with the assignment. The classification system proposed here is broadly applicable and standardized,

ACPD
13, 983–1044, 2013

so that it is portable across many systems. This taxonomy will be useful as a common ground for discussion of heterogeneous chemical processes and as a tool for analysis.

2 Conceptual framework

2.1 Representation of aerosol reaction systems and definitions

Following the terminology of Pöschl et al. (2007) (the "PRA framework"), we will discuss the reaction of a trace gas species X and a condensed-phase substrate Y. These compounds are assumed to react in a single step, second-order reaction in either (i) a single bulk layer or (ii) between a quasi-static surface layer of Y and a sorption layer of X. The domains of the gas and condensed phase discussed here are illustrated schematically in Fig. 1 along with the principle mass transport and reaction processes.

In this paper we reserve the term *limiting case* for a system which is governed by a single, clearly defined rate-limiting process. Examples of limiting cases are systems which are limited solely by slow chemical reaction, or by slow diffusion of reactants X and Y. We reserve the term *kinetic regime* for a system which is governed by a few (often only one or two) clearly defined rate-limiting processes. For example, systems which exhibit reaction and/or bulk diffusion limitation fall into a single kinetic regime. Referencing the concepts of reacto-diffusive length and flux (Schwartz and Freiberg, 1981; Hanson et al., 1994; Pöschl et al., 2007), we term this important example the reaction-diffusion regime.

2.2 Derivation of limiting cases and kinetic regimes

The cases of limiting behavior presented here arise from three properties that are fundamental to every aerosol reactive system in which a gas X reacts with condensed phase Y:

ACPD
13, 983–1044, 2013

(i) the reaction location, as assessed by the Surface to Total Loss rate Ratio (STLR)

(ii) the supply of reactive gas, as assessed by the Saturation Ratio (SR)

(iii) the heterogeneity of the system with respect to depth above and below the surface, as assessed by the Mixing Parameter (MP).

Each of the three quantities (STLR, SR, MP) is formulated as a dimensionless parameter ranging from 0 to 1 to allow comparison against a common set of criteria which are not linked to any specific chemical reaction.

Every unique combination of extreme behavior in the three classification properties leads to a limiting case. This can be visualized in three dimensions as a cube in which each dimension corresponds to one of the classification properties, as shown in Fig. 2. Since all possible cases of kinetic behavior form the interior of the cube and the faces describe extreme behavior in one of the classification properties, the eight limiting cases can be depicted as a small volume at each of the vertices, touching three faces each. The eight cases obtained in this way are limited by a single process each and are clearly distinct since they differ in at least one fundamental classification property.

To facilitate discussion, we introduce a compact symbolic representation for each limiting case which is used in Fig. 2 and throughout this manuscript. The reaction location is indicated by a central "S" or "B" for surface and bulk respectively, and a subscript indicates the process which limits reactive uptake. The possible subscripts are: "rx" to indicate the reaction rate; "bd" to indicate bulk diffusion; "α" to indicate accommodation; "gd" to indicate gas-phase diffusion. This framework thus distinguishes four different types of limitation, which are color-coded in Fig. 2.

A particular strength of numerical modeling (either depth-resolved models or numerically solved resistor models) is the ability to work in the "gray area" between well-defined limiting cases. The framework proposed here is compliant with systems in which one or two classification parameters do not exhibit extreme behavior: these fall into the kinetic regimes defined above. In order to illustrate the concept of a kinetic

ACPD
13, 983–1044, 2013

regime, a few of the many possible regimes are shown in Fig. 3. A straightforward way to generate a regime is to connect the volume which represents two limiting cases to form a volume, which also contains the additional space between the limiting cases and towards the center of the cube. The resulting regime includes the behavior of both limiting cases and all systems with classification parameters located in the additional volume and is thus much broader in its definition. This is depicted in Fig. 3b, where surface and bulk reaction limiting cases with the same limiting process (boxes of the same color) are connected. We name the four resulting regimes for the process which limits the reactive loss of Y: the reaction, bulk diffusion, gas diffusion and accommodation regimes.

Another possibility is shown in Fig. 3a, where the reaction and bulk diffusion regimes are linked to form a reaction-diffusion regime. This reaction-diffusion regime thus includes systems which are limited by reaction, bulk diffusion, or both processes in situations where they are tightly coupled (reacto-diffusive limitation). We note that the term "reacto-diffusive" traditionally referred to bulk reaction systems with a strong gradient in X and no gradient in Y (see e.g. Danckwerts, 1951; Schwartz, 1986; Hanson et al., 1994; Davidovits et al., 1995; Ravishankara, 1997; Kolb et al., 1998; Ravishankara and Longfellow, 1999; Davidovits et al., 2006; Pöschl et al., 2007; Kolb et al., 2010). Throughout this paper, we will refer to this case as the "traditional reacto-diffusive case." However, our definition of the reaction-diffusion regime also includes cases with gradients in the bulk material Y in both bulk and surface reaction systems. In these systems, a reacto-diffusive steady state forms when both the diffusion of reactants towards the reaction site and the actual reaction rate are limiting trace gas uptake. The complementary regime is a combination of the accommodation and gas diffusion regimes, which we will refer to as the "mass-transfer" limited regime as both are related to the transfer of X from the gas to the particle phase.

To facilitate discussion of regimes, we introduce additional symbols which are similar to that of the limiting cases defined above. Again, "S" and "B" are used to indicate reaction location, and superscripts are used to avoid confusion in identifying the rate-limiting

ACPD
13, 983–1044, 2013

processes. Additional possible superscripts are "rd" to indicate reaction-diffusion limitation and "mt" to indicate mass-transfer limitation. In the case that STLR does not have extreme behavior, a regime can still be specified if the other classification parameters are consistent. For example, if STLR is ~ 0.5 but SR indicates that the saturation ratio is high, we can assign the behavior as SB^{rd}, where the central symbol is SB to indicate that both surface and bulk reactions contribute. The traditional reacto-diffusive case as defined above (bulk reaction, gradient only in X) will be denoted as B^{rd}_{trad} to distinguish it from the broad manifold of possible behaviors encompassed in our reaction-diffusion regime, SB^{rd}. In addition to the regimes already presented here, a variety of other regimes are possible; a few of them are documented in Appendix B.

2.3 Classification scheme and criteria

Here we present a sequential method to apply the three parameters defined above to unambiguously determine the limiting case of a reacting aerosol particle. These classification parameters will be described in detail in Sects. 2.3.1–2.3.3. An overview of the process is given in Fig. 4 and the resulting limiting cases and kinetic regimes are summarized in Table 1.

In the following sections, each of the three classification parameters is framed as a question to provide insight into the processes which most strongly influence the gas uptake. It is important to note that multiple functional forms of SR and MP exist; one of each is chosen for use depending on the result of the previous classification parameters. For example, the mixing parameter for a reaction which occurs primarily at the surface should not reflect a depthwise gradient in bulk X.

A conceptual discussion of the physical and chemical behavior of each limiting case is possible without appealing to any specific numerical model, but the process of calculating parameter values to assign a limiting case for some experimental data requires the output of a depth-resolved model. The criteria are constructed assuming that model outputs are discretized into spherical or planar layers for droplets and films respectively, as such discretized treatment is common in current-generation models (see Fig. 1).

ACPD
13, 983–1044, 2013

2.3.1 Criterion 1: surface to total loss rate ratio (STLR)

This term answers the question: *What is the dominant reaction location, surface or bulk?* The Surface to Total Loss rate Ratio (STLR) is used to determine which locality, if any, dominates the chemical loss of Y. The loss rates at the surface, L_s and in the kth bulk layer, L_{bk}, can be calculated as follows:

$$L_s = k_{SLR}[X]_s[Y]_{ss} \quad (1)$$

$$L_{bk} = k_{BR}[X]_{bk}[Y]_{bk} \quad (2)$$

Here k_{SLR} and k_{BR} are the second-order reaction rate coefficients in the bulk and in the surface layer, respectively, [X] and [Y] are the concentrations of the reactants and the subscripts s, ss, and bk indicate the sorption layer, the quasi-static surface layer, and the kth bulk layer respectively (see also Fig. 1 above). For a total of n bulk layers, the STLR can then be calculated as:

$$\mathrm{STLR} \equiv \frac{L_s}{L_s + \sum_{k=1}^{n} L_k} \quad (3)$$

In Fig. 4, the STLR decision distinguishes the surface (left half) from the bulk cases (right half). The numerical interpretation of STLR is

1. As STLR approaches zero, the reaction occurs primarily in the bulk.
2. As STLR approaches unity, the reaction occurs primarily at the surface.

2.3.2 Criterion 2: saturation ratio (SR)

This term answers the question: *Is the supply of external gas limiting the reaction rate?* This criterion classifies particles by the abundance of X at the surface or in the first bulk layer, and is thus used as a proxy for the balance between supply of X (from the gas phase) and loss of X (by desorption, surface reaction, bulk reaction, and diffusion

ACPD
13, 983–1044, 2013

into the bulk) in those locations. In Fig. 4, this decision step distinguishes the reaction-diffusion regime with high SR (top, SB^{rd}) from the mass-transfer regime with low SR (bottom, SB^{mt}). In both the surface and the bulk case detailed below, the actual concentration of X in the locale where reaction occurs is compared to the saturation value of X which would be achieved in the absence of reacto-diffusive loss, leading to a direct determination of which regime a system expresses, reaction-diffusion limitation or mass-transfer limitation.

SR in surface-reaction dominated cases

In cases where surface reaction dominates (STLR ≈ 1), the SR is calculated as the Surface Saturation Ratio (SSR). With this parameter, the surface concentration of X is compared to the surface saturation concentration $[X]_{s,sat}$. In the absence of reaction or diffusion into the bulk, the saturation concentration of X at the surface is determined by the rates of adsorption and desorption k_a and k_d:

$$[X]_{s,sat} = \frac{k_a}{k_d} \cdot [X]_{gs} = K_{ads,X} \cdot [X]_{gs} \quad (4)$$

Here $[X]_{gs}$ is the near-surface gas-phase concentration of X and $K_{ads,X}$ is a Langmuir-type adsorption equilibrium constant (see Fig. 1). The SSR is defined as the ratio of X to its saturation concentration at adsorption equilibrium:

$$SSR = \frac{\theta_{s,X}}{\theta_{s,sat,X}} = \frac{[X]_s}{[X]_{s,sat}} \quad (5)$$

where $\theta_{s,X}$ is surface coverage as defined in Pöschl et al. (2007) and $\theta_{s,sat,X}$ (not to be confused with $\theta_{s,max} = 1$) is the saturation coverage achievable at the equilibrium surface concentration defined in Eq. 4.

ACPD
13, 983–1044, 2013

SR in bulk-reaction dominated cases

In cases where bulk reaction dominates (STLR ≈ 0), the SR is calculated as the Bulk Saturation Ratio (BSR). In this parameter, the concentration of X in the first subsurface bulk layer ($[X]_{b1}$) is compared to the saturation concentration ($[X]_{b,sat}$) achievable under equilibrium conditions in the absence of reacto-diffusive loss:

$$BSR = \frac{[X]_{b1}}{[X]_{b,sat}} \quad (6)$$

Here we suggest that $[X]_{b,sat}$ should be defined in terms of the Henry's law equilibrium constant and the gas-phase concentration $[X]_g$.

The numerical interpretation common to both SR is:

1. As SR approaches zero, the system is starved of X and is mass-transfer limited (SB^{mt} regime).

2. As SR approaches unity, the system is adequately supplied with X and experiences reaction-diffusion limitation (SB^{rd} regime).

2.3.3 Criterion 3: mixing parameters (MP)

This term answers the question: *What is limiting the reaction rate: mixing or chemistry?* Much of the additional information in depth-resolved models is included in the parameter set which represents the spatial heterogeneity in the system. In the case of a surface reaction, a slow diffusion of Y to the surface may hinder the reaction, while in the bulk, reaction speed may be limited by the diffusion of X and possibly the diffusion of Y. In mass-transfer limited systems, only mixing in the gas phase has to be considered. Thus three different Mixing Parameters (MP) are used to assess mixing in reacting particles: (i) The surface mixing parameter of Y, SMP_Y, for reaction-diffusion limited surface reaction systems (S^{rd}); (ii) the bulk mixing parameter of X and Y, BMP_{XY},

ACPD
13, 983–1044, 2013

for reaction-diffusion limited bulk reaction systems (B^{rd}) and (iii) the gas-phase diffusion correction factor, $[Y]_{g,X}$, for mass-transfer limited systems (SB^{mt}). In Fig. 4, this classification step divides the reaction-diffusion and mass-transfer limited regimes each into well-mixed cases (top half) and cases which are limited by bulk or gas-phase gradients (bottom half).

MP in surface reaction-diffusion limited systems

In surface reaction-diffusion limited systems (S^{rd}, STLR ≈ 1, SSR ≈ 1), the reaction rate may be limited by the availability of Y at the surface. Assuming that Y is non-volatile, a deficit in Y at the surface is caused by reaction with X and incomplete mixing with the particle bulk. Thus we define SMP_Y as the ratio of the actual surface concentration $[Y]_{ss}$ to the maximum possible surface concentration $[Y]_{ss,max}$:

$$SMP_Y = \frac{[Y]_{ss}}{[Y]_{ss,max}}. \quad (7)$$

Here we propose $[Y]_{ss,max} = [Y]_{bn} \times \delta_Y$, namely that the maximum possible surface concentration of Y should be linked to the bulk concentration at the center of the particle (layer n) and a geometric factor δ_Y to relate the molecular volume concentration (cm^{-3}) to the molecular area concentration (cm^{-2}). Referencing the surface concentration against the innermost bulk layer gives maximum sensitivity to depthwise gradients in Y. It is important to note that the maximum surface concentration $[Y]_{ss,max}$ may change as the reaction proceeds due to decreased abundance of Y in layer n.

The numerical interpretation of SMP_Y is:

1. As SMP_Y approaches zero, a strong gradient in Y exists from the center of the bulk to the surface of the particle, and the system is in the S_{bd} limiting case.

2. As SMP_Y approaches unity, Y is well-mixed throughout the particle and the system is in the S_{rx} limiting case.

ACPD
13, 983–1044, 2013

MP in bulk reaction-diffusion limited systems

In bulk reaction-diffusion limited systems (B^{rd}, STLR ≈ 0, BSR ≈ 1), a gradient in X and/or Y may limit the reaction rate, so that expressions for both the mixing of X and Y in the bulk are needed. For both species, the reacto-diffusive length will be compared to the particle size to assess the degree of mixing. In general, the reacto-diffusive length is the depth-wise distance over which the concentration of a material decreases to $1/e$ of its original value. The reacto-diffusive length will increase as the diffusivity of the material increases and will decrease as the reaction rate coefficient becomes higher. For compounds X and Y which react with one another, the reacto-diffusive length can be expressed as:

$$l_{\mathrm{rd,X}} = \sqrt{\frac{D_{\mathrm{b,X}}}{k_{\mathrm{BR}} \times [\mathrm{Y}]_{\mathrm{eff}}}} \tag{8}$$

$$l_{\mathrm{rd,Y}} = \sqrt{\frac{D_{\mathrm{b,Y}}}{k_{\mathrm{BR}} \times [\mathrm{X}]_{\mathrm{eff}}}} \tag{9}$$

where $[\mathrm{X}]_{\mathrm{eff}}$ and $[\mathrm{Y}]_{\mathrm{eff}}$ are the effective concentrations of X and Y in the region where the reaction occurs and $D_{\mathrm{b,X}}$ and $D_{\mathrm{b,Y}}$ are the diffusion constants of each material in the bulk matrix. This formulation is needed in the case of a strong depth-wise gradient in the reaction partner, in which case the simple average concentration might be misleading. Specifically, we propose that the effective concentration should be calculated as the volume- and loss rate-weighted concentration:

$$[\mathrm{X}]_{\mathrm{eff}} = \frac{\sum_{k=1}^{n} L_{\mathrm{k}} \times V_{\mathrm{k}} \times [\mathrm{X}]_{\mathrm{bk}}}{\sum_{k=1}^{n} L_{\mathrm{k}} \times V_{\mathrm{k}}} \tag{10}$$

$$[\mathrm{Y}]_{\mathrm{eff}} = \frac{\sum_{k=1}^{n} L_{\mathrm{k}} \times V_{\mathrm{k}} \times [\mathrm{Y}]_{\mathrm{bk}}}{\sum_{k=1}^{n} L_{\mathrm{k}} \times V_{\mathrm{k}}} \tag{11}$$

ACPD
13, 983–1044, 2013

where V_k is the volume of the kth layer. This definition of the effective concentration of the reaction partner in the zone where the reaction occurs allows the use of the reacto-diffusive length of each species to gauge the degree of mixing of X and Y within the particle.

We define the BMP_X and BMP_Y, the bulk mixing parameters for X and Y respectively, to be:

$$BMP_X = \frac{l_{rd,X}}{l_{rd,X} + \frac{r_p}{e}} \quad (12)$$

$$BMP_Y = \frac{l_{rd,Y}}{l_{rd,Y} + \frac{r_p}{e}} \quad (13)$$

so that both BMPs approach unity as their reacto-diffusive length becomes much larger than the particle radius r_p and approach zero as their reacto-diffusive length becomes much smaller than the particle radius. In BMP_X and BMP_Y, we have chosen to scale the particle radius by $1/e$ to be consistent with the e-folding characteristic of the reacto-diffusive length.

Finally, as the presence of a gradient in only one compound is insufficient to drive a system into the B_{bd} limiting case, we define BMP_{XY} as the average of BMP_X and BMP_Y:

$$BMP_{XY} = \frac{BMP_X + BMP_Y}{2} \quad (14)$$

The numerical interpretation of BMP_{XY} is:

1. As BMP_{XY} approaches zero, strong gradients in both X and Y limit loss rate and the system is in the B_{bd} limiting case.

2. As BMP_{XY} approaches unity, X and Y are well-mixed throughout the particle and the system is in the B_{rx} limiting case.

ACPD
13, 983–1044, 2013

A gradient solely in X is insufficient to cause bulk diffusion limitation and thus to bring about a B_{bd} limiting case classification. For details and justification see appendix C.

MP in mass-transfer limited systems

For either bulk or surface reactions (any value of STLR), there are two scenarios which lead to mass-transfer limitation (SSR and/or BSR ≈ 0): either trace gas reactant X is depleted in the near-surface gas phase (see Fig. 1) or the accommodation process is inefficient. This distinction is important as in the second case a physical or chemical change in the system might result in increased accommodation efficiency, leading to significant changes in reaction system behavior. A simple and physically meaningful metric to distinguish these two cases is the gas-phase diffusion correction factor for uptake by aerosols (Pöschl et al., 2007), $C_{g,X}$, which we take as the gas-phase mixing parameter.

$$C_{g,X} = \frac{[X]_{gs}}{[X]_g} = \frac{1}{1 + \gamma_X \frac{0.75+0.28\ Kn_X}{Kn_X(1+Kn_X)}} \tag{15}$$

As can be seen, $C_{g,X}$ can be calculated in two ways, either directly via model output of $[X]_{gs}$ and $[X]_g$, which are the trace gas concentrations near the surface and far from the particle, respectively; or via model output of γ_X and Kn_X, which are the net uptake coefficient of X and the Knudsen number of the diffusive system. The Knudsen number (see Pöschl et al., 2007) is the ratio of the mean free path of the trace gas molecule λ_X to the particle radius, where λ_X depends on the gas-phase diffusivity $D_{g,X}$ and the mean thermal velocity of the gas ω_X ($\lambda_X \approx 70$ nm at atmospheric pressure for ozone) so that

$$Kn_X = \frac{\lambda_X}{r_p} = \frac{3\ D_{g,X}}{r_p\ \omega_X}. \tag{16}$$

The numerical interpretation of $C_{g,X}$ is:

ACPD
13, 983–1044, 2013

1. As $C_{g,X}$ approaches zero, the system shows a strong spatial gradient in $[X]_g$ and the system is limited by diffusion of gas phase X to the particle surface.

2. As $C_{g,X}$ approaches unity, no spatial concentration gradient exists in $[X]_g$ and the system is therefore limited by accommodation.

3 Examples of atmospheric relevance

The limiting cases described above are meant to provide a conceptual framework for chemical kinetics in atmospheric particles and allow physical and chemical intuition to be applied in a complex system. A few examples of well-known systems which fall into well-defined limiting cases are the following:

3.1 Well-mixed bulk reaction systems [B_{rx}]

Many of the slow aqueous phase reactions fall into this limiting case, which arises when both X and Y are plentiful and ubiquitous throughout the particle. This is the case for the reaction of O_3 with SO_2 under acidic conditions (where formation of HSO_3^- or SO_3^{2-} is not likely, cf. Seinfeld and Pandis, 2006), the self-reaction of HO_2 in absence of transition metal ions (cf. Abbatt et al., 2012, and references therein, especially George et al., 2011), or reactions involving NO_2 (Ammann et al., 2005). Such reactions are typically not a major sink of the trace gas involved from the gas phase, but are important in terms of aerosol aging if they are the principle transformation of the condensed phase compound.

3.2 Well-mixed surface reaction systems [S_{rx}]

Many relevant reactions on solid surfaces, such as ice, mineral dust, or soot fall into this limiting case (e.g. surface oxidation of polycyclic aromatic hydrocarbons by ozone, Shiraiwa et al., 2009). Moreover, gas uptake by liquid aqueous substrates can also be

ACPD
13, 983–1044, 2013

limited by surface reaction rate. For example, the reaction of Cl_2 with Br^- has a strong surface component, especially at low Cl_2 gas-phase concentrations (Hu et al., 1995). Similarly, Knipping et al. (2000) as well as Knipping and Dabdub (2002) suggested a surface reaction between the OH radical and Cl^- under atmospheric conditions via formation of a surface complex (Laskin et al., 2003; Shaka' et al., 2007).

3.3 Mass-transfer limited systems [S_α, B_α; S_{gd}, B_{gd}]

Surface accommodation limitation necessarily occurs during the equilibration of fresh surface upon exposure to X, e.g. HCl on H_2SO_4 (Morris et al., 2000; Behr et al., 2001, 2009), but also for all other surface precursor mediated processes mentioned above. If transfer into aqueous droplets is fast, bulk accommodation is rate limiting until solubility equilibrium begins to limit uptake. For soluble gases, this may be the dominant case for uptake into the aqueous phase in clouds. Each of the accommodation limited cases mentioned above may become gas-phase diffusion limited as the particle becomes sufficiently large (and *Kn* becomes small). This may be important in laboratory experiments with supermicron droplets and for cloud droplet or aerosol growth.

3.4 Bulk-diffusion limited systems [S_{bd}, B_{bd}]

In the past, reactions in atmospheric aerosols were assumed to occur in well-mixed droplets with no limitation due to diffusion in the condensed phase. However, recent evidence shows that aqueous particles may transition into highly viscous semi-solid or glassy states (Zobrist et al., 2008; Koop et al., 2011; Virtanen et al., 2010), which lead to strong diffusional limitations on reaction rate. Diffusion of one or both reactants in the bulk may become rate limiting. Examples include the nitration of amorphous protein (Shiraiwa et al., 2011a, 2012c), the reaction of NO_3 with levoglucosan (Shiraiwa et al., 2012b), and (non-reactive) uptake of water to dissolve a glassy aerosol (Mikhailov et al., 2009; Zobrist et al., 2011; Koop et al., 2011; Tong et al., 2011).

ACPD
13, 983–1044, 2013

3.5 Changes in kinetic behavior as a function of time and ambient conditions

Each of the examples given above references a single limiting case, and in many cases the limiting case or regime assignment may remain constant throughout the majority of a reaction. However, the limiting case or kinetic regime will almost certainly change in the first moments of reaction or as reaction products accumulate. For example, in a bulk reaction dominated system, the uptake of soluble trace gases into liquid particles could be initially accommodation-limited (B_α) and thereafter pass into B_{bd} for viscous droplets or into B_{rx} for slow bulk phase reactions. This demonstrates that a system may evolve from one limiting case to another in time. Although time-invariant kinetic parameters are used in the case study of oleic acid – ozone in Sect. 6, the classification system described here is compliant with temporally varying parameters such as changing bulk diffusivities $D_{b,X}$ and $D_{b,Y}$ as a reaction proceeds (e.g. as in Pfrang et al., 2011). This might occur when reaction products alter the viscosity of the bulk matrix. The classification framework is also independent of model choice; a model that explicitly treats product formation along with evaporation of volatile products could be used with the framework as proposed above.

In addition to noting that the kinetic behavior will change as the reaction proceeds, we caution against the logical error of assuming that the kinetic regime or limiting case observed in one experiment will be the same under ambient conditions or in another experiment under different conditions. For this reason, we recommend that the limiting case for an aerosol system under ambient conditions should be calculated as part of a standard analysis, espeically if experimental conditions are significantly different than ambient. For example, the reaction of ozone with bromide (a potentially important reaction for the liberation of halogens out of aqueous sea-salt) is dominated by a surface reaction (S_{rx}) at atmospherically relevant ozone concentrations, while it is dominated by a bulk reaction (B_{rx}) at very high ozone concentration (Oldridge and Abbatt, 2011).

ACPD
13, 983–1044, 2013

4 Numerical modeling of limiting cases

Up to this point, the limiting cases and regimes have been described in terms of trends in the parameters, but the actual assignment of a reaction system to a limiting case requires a set of numerical criteria and a model to generate the time- and depth-resolved data. In this section we describe our choice of depth-resolved model and propose a set of numerical criteria for differentiation of aerosol behavior along with a global sensitivity analysis method to confirm that the numerical criteria result in distinct limiting cases.

4.1 KM-SUB model description and method

In the following analyses, we have chosen to employ the KM-SUB model of Shiraiwa et al. (2010) but this set of limiting cases and classification criteria could be used with any model which produces time- and depth-resolved outputs. KM-SUB is a kinetic model that treats mass transport and chemical reaction at the surface and in the bulk of aerosol particles. It follows the nomenclature of the PRA framework and consists of model compartments as outlined in Sect. 2.1 and shown in Fig. 1. KM-SUB solves a set of ordinary differential equations for the flux-based mass balance to and from each layer, resolving the following processes: gas-phase diffusion, adsorption and desorption onto the particle surface, surface-bulk exchange, bulk diffusion of trace gas and bulk material as well as surface and bulk reactions. The original gas-phase diffusion correction term in KM-SUB was replaced by an explicit near-surface gas-phase layer (following the treatment of gas flux through a virtual surface, found in Eq. 12 of Pöschl et al., 2007). Effectively, the kinetic behavior of a physical system is described in this modified version of KM-SUB by the eight parameters given in Table 2 (not including experimental observables such as r_p, $[X]_g$, etc.). The number of layers calculated by the model was adjusted until model results converged to ensure adequate depthwise resolution.

The KM-SUB model was used to calculate idealized limiting case profiles which are not tied to any specific chemical system (see Sect. 5.1) and also to simulate the re-

ACPD
13, 983–1044, 2013

action of oleic acid – ozone for the experimental conditions of Ziemann (2005), Lee and Chan (2007) and Hearn et al. (2005) in Sect. 6. Because the limiting case is likely to change one or more times upon the onset of reaction (see Sect. 3.5), it is necessary to determine the limiting case at a specific point in time or at a specific point in the reaction. Our experience shows that limiting behavior tends to be stable over long parts of the experiment after the initial rapid changes. As the KM-SUB model does not explicitly treat the products of this reaction, limiting cases were assigned at the point where 50 % of the initial reactant Y was consumed using the numerical criteria of Sect. 4.2. However, in these experiments the limiting case assignments are the same if the assignment is made at either 10 % or 50 % reaction course (see Table 6 below), so comparison with previous studies which used initial rate methods is possible.

4.2 Numerical criteria and partially defined behavior

Even though a system may exhibit steady state reactivity over a long period of time, the situation cannot be necessarily assigned to one of the limiting cases. An ideal system would have binary behaviors (e.g. only surface or bulk reactions, but not both), but in real systems some mixed character is expected. The ability to assign a limiting case (or lack thereof) is thus a consequence of the physical system under study and the conditions of each experiment. The exact positions of such boundaries for limiting cases and regimes are rather subjective and may change depending on the application. Here, we employ a 9:1 criterion for limiting cases, such that at least 90 % of the behavior is represented by the kinetic regime definition at each classification step. The boundaries for regimes are more relaxed at 3:1 criteria, so that more space can be classified. Although knowledge of the system's kinetic regime is less valuable than the confirmation of (single-process) limiting behavior, such a classification might still be useful. Prominent examples of systems which could be classified by a regime but not a limiting case are heterogeneous kinetics in the bulk reaction-diffusion kinetic regime (B^{rd}), such as the reaction of HCl with HOCl in sulfuric acid solutions (Hanson and Lovejoy, 1996; Donaldson et al., 1997, and references therein), the hydrolysis of

ACPD
13, 983–1044, 2013

$ClONO_2$ (Deiber et al., 2004), or the reaction of O_3 with iodide (Rouvière et al., 2010). In these examples, kinetic regimes can help by providing a less stringent classification than a limiting case. However, unless the numerical criteria are set at 1:1 with no unspecified region, there will be some combinations of classification parameters for which no assignment is possible.

4.3 Global sensitivity analysis

The best indication that an assignment to a limiting case is justified and that the choice of numerical criteria is sufficiently strict is given by a sensitivity analysis which confirms that (i) the system is controlled by a single process and (ii) responds appropriately to changes in input parameters (e.g. S_α cases should depend only on the surface accommodation coefficient $\alpha_{s,0}$ and not on the surface reaction rate coefficient k_{SLR} etc.). In general, sensitivity towards an input parameter λ_i can be expressed through its sensitivity coefficient $S(\lambda_i)$, which may be defined as

$$S(\lambda_i) = \left(\frac{\Delta Y_{model}}{\Delta \lambda_i}\right). \quad (17)$$

However, the values of S_i cannot be compared directly because they depend on the magnitudes of the input parameters (λ_i) which are being varied and the observed model output Y_{model}. Thus we employ a normalized sensitivity coefficient (following Saltelli et al., 2008) which allows the influence of input parameters to be directly compared:

$$S^n(\lambda_i) = \frac{\frac{1}{Y_{model}}\partial Y_{model}}{\frac{1}{\lambda_i}\partial \lambda_i} = \frac{\partial \ln(Y_{model})}{\partial \ln(\lambda_i)} \quad (18)$$

For the computation of sensitivity coefficients we employ a variation on the Elementary Effects (EE) Method as proposed by Morris (1991). The EE method is a simple global screening method that uses a one-at-a-time sampling approach (other approaches are

ACPD
13, 983–1044, 2013

also possible, for a summary see e.g. Saltelli et al., 2008). The method follows a randomly generated trajectory through input parameter space, and records the changes in model output Y_{model} due to changes in each input parameter λ_i. Only one parameter is varied at each step, and all previous changes are kept, which leads to generation of a full set of local sensitivity coefficients. To account for biases due to the random trajectory generation, a large number of trajectories are generated and a representative sample is chosen so that the entire input parameter space is adequately represented. The global sensitivity coefficient is thus finally obtained by taking the arithmetic mean μ_i of all computed local values. The associated standard deviation σ_i is a measure for interactions between and non-linearity of the input parameters λ_i.

In this study, we use the total loss rate, TLR = $L_s + \sum_k L_k$ as model output characteristic for the reaction system. The result of this analysis is a set of normalized sensitivity coefficients, which indicate the strength of the model response to changes in each input parameter. Crucially, this sensitivity analysis is only possible in the context of a specific chemical system, physical size (distribution) of aerosol particles, and for a given set of kinetic constants. For this study we perform sensitivity analyses in the context of the oleic acid – ozone system (see Sect. 6.5 below), but recommend the analysis to be performed for each new system to ensure that appropriate numerical limits are chosen. Even within the same chemical system with the same kinetic constants, the calculated sensitivities will change in response to differing experimental conditions such as gas-phase oxidant concentration or particle size.

The interpretation of the normalized sensitivity coefficients can be achieved by connecting the input parameter λ_i to the original model output Y_{model} by the power law relationship:

$$Y_{\text{model}} \propto \lambda_i^{S^n(\lambda_i)}. \tag{19}$$

In words, this indicates that the model output responds to changes in input parameter λ_i in proportion to the $S^n(\lambda_i)$th power of the change. For example, a $S^n(\lambda_i)$ of −1 would indicate inverse dependence on input parameter λ_i etc.

ACPD
13, 983–1044, 2013

5 Identification of limiting cases and scaling from laboratory to ambient conditions

The limiting cases and regimes described above are essentially statements of which underlying processes are most influential to a reaction for a given set of conditions. As such, they have the potential to aid experimental planning by suggesting which parameters should be adjusted to maximize experimental effectiveness. If the underlying kinetic parameters such as reaction rate coefficients and diffusivities are extracted from experimental data, these parameters would provide direct insight into the physicochemical processes at work in the system and are portable to different conditions.

However, the kinetic parameters of a system can only be available after comprehensive studies, often requiring multiple experiments. Without these parameters it is not possible to perform calculations with a depth-resolved model to make an immediate assignment of limiting case or regime behavior. Fortunately, the limiting cases display some characteristic behaviors which can provide insight into the reaction system from experimental observables (e.g. reactive uptake coefficient as a function of time) and from responses to controlled variables (e.g. change in reactive uptake coefficient as a function of r_p or $[X]_g$). In this section we will present the characteristic behaviors of the limiting cases and summarize how each limiting case behaves with respect to time, r_p, and $[X]_g$, which will allow an experimentalist to narrow the list of possible limiting cases by visual inspection of experimental data and possibly plan future experiments based on those conclusions.

In particular, the sensitivity coefficients given in Sect. 5.2 provide an indication of how experimental results will change as a function of time or other experimentally controllable factors like r_p or oxidant concentration. In the discussion that follows we will give special attention to the interchangeability of time and oxidant concentration, which is a necessary condition for usage of the net exposure metric (concentration of oxidant × time) for application to atmospheric concentrations and time scales. Renbaum and Smith (2011) recently showed that under constant precursor concentrations, the expo-

ACPD
13, 983–1044, 2013

sure metric was valid for the reaction of OH and Cl radicals with squalane, brassidic acid, and 2-octyldodecanoic acid. However, other studies have found that the exposure metric breaks down when scaling from laboratory to ambient conditions, as summarized by Renbaum and Smith (2011).

5.1 Characteristic decay shapes

An overview of the eight distinct limiting cases and several regimes is given in Table 3 along with their characteristic limiting process(es). Each limiting case has a single rate-limiting process by definition and exhibits a characteristic behavior as a function of time. A set of idealized KM-SUB parameter sets has been obtained by modifying the typical base case for the reaction oleic acid and ozone, assuming that all kinetic (e.g. k_{BR}, $D_{b,X}$, $D_{b,Y}$) and environmental (e.g. $[X]_g$, r_p, T) parameters remain constant as the reaction proceeds. The complete list of input parameters and experimental conditions for these cases is given in Tabs. S2 and S3. Single-process limitation was ensured by disabling competing processes ($\lambda_i = 0$) and increasing the speed of non-limiting processes ($\lambda_i = 1$). To achieve similar uptake coefficients, the kinetic parameters were tuned so that an aerosol particle with 100 nm radius was processed in ~100 s. The parameter sets themselves are thus not based on physically correct scenarios, but represent systems which exhibit pure, single process limiting behavior.

The computed behaviors for archetypal limiting cases are shown in Fig. 5 as a function of time for the total number of molecule Y remaining ($N_Y = \sum_{k=1}^{n}[Y]_{bk} \times V_k$) and for the effective uptake coefficient ($\gamma_{eff,X} = \gamma_X \times C_{g,X}$). These two quantities represent the observable for experimental apparatus which monitors bulk Y (N_Y) or gas-phase X ($\gamma_{eff,X}$). Data for N_Y are shown on a linear time axis with linear (Fig. 5a) and logarithmic (Fig. 5b) y-axes. Data for $\gamma_{eff,X}$ are shown on a logarithmic y-axis with a linear (Fig. 5c.) and logarithmic (Fig. 5d) time axis. All N_Y data are normalized against its initial value of $N_{Y,0}$ and all time data are scaled to t_{99} (the time at which 99 % of the bulk material has reacted). We will discuss the limiting case behaviors by grouping them according to their appearance in Fig 5a: (i) linear, and (ii) non-linear.

ACPD
13, 983–1044, 2013

Linear decay behavior in N_Y, as can be seen for the S_α, B_α, S_{gd}, B_{gd} limiting cases in panel a, arises when transport over a certain interface creates a bottle-neck that limits the reaction (effectively, a 0th order-type reaction). In panels c and d, these behaviors are characterized by time-invariant values of $\gamma_{eff,X}$. As opposed to panels a and b, not all lines with similar shape are overlapping since reaction speeds slightly differ between the chosen input parameter sets and no normalization for $\gamma_{eff,X}$ has been carried out. However, the qualitative lineshape is consistent, independent of the actual reaction speed.

Among non-linear behaviors, the most easily recognized is the mono-exponential decay behavior in N_Y, which has a linear profile in the logarithmic panel b. This is true for for S_{rx} and B_{rx} cases, in which the concentration of X at the reaction site remains nearly constant, leading to a pseudo-first-order type reaction. The S_{bd} limiting case shows nearly-linear behavior in panel b after an initial period of fast decay, an indication that the system is not a true S_{bd} limiting case in the first moments of the reaction as the gradient in Y has yet to develop. Panel c shows the according linear decrease of $\gamma_{eff,X}$ in time for these three cases, again with a higher initial uptake for the S_{bd} case. The initial decay of $\gamma_{eff,X}$ for the S_{bd} case is well-resolved in panel d, showing a linear decrease in log-log space with slope $\frac{1}{2}$. This is characteristic for cases that are not in reacto-diffusive steady state, an inherent property of bulk diffusion limited cases.

The same initial decay of $\gamma_{eff,X}$ can thus be found for the B_{bd} case. This case furthermore shows a non-linear, higher-order exponential decay in N_Y as can be seen from panels a and b. The reaction slows down significantly once the diffusional gradients in X and Y are developed. As the rate of formation of the gradients and the location where the gradients form is not prescribed, this limiting case is expected to encompass a range of behaviors and will not have a single defining characteristic.

In addition to the eight limiting cases, the B^{rd}_{trad} special case can be recognized by showing a quadratic decay of N_Y as a function of time in linear space (a). In panel d, it resembles the S_{rx} and B_{rx} cases, but can be distinguished from those two in the linear representation, panel c.

ACPD
13, 983–1044, 2013

5.2 Scalability of each limiting case

The typical response of each limiting case to changes in $[X]_{gs}$ and r_p was investigated using the global sensitivity method described in Sect. 4.3 and the results are given in Table 4. The standard kinetic method of performing "experiments" (here, simulations) at differing $[X]_g$ and r_p to determine the response (linear, inverse, etc.) yielded identical results when the cubic dependence of N_Y on r_p was taken into account. The results of the sensitivity analysis performed on the limiting cases displayed above indicate that the exposure metric is acceptable to use (i.e. linear response to $[X]_g$, $S^n([X]_g) = 1$) as long as a transport process is not saturated.

In the example of S_{rx} behavior above, all surface sites were occupied ($\theta_{s,sat} = \theta_{s,max} = 1$ and $\theta_s \approx \theta_{s,sat}$) and thus changes in $[X]_g$ had no effect on the reaction rate. In this situation, it is typical that the measured uptake coefficient γ_X is inversely proportional to $[X]_g$. Thus in addition to the explanations already offered for failures of scalability (e.g. secondary chemistry, absorption of other gases, etc.), we suggest that systems in which the transport from gas to the reaction site at or in the particle is rate limiting (i.e. B_{bd} and S_{bd} behavior as well as S_{rx} with $\theta_{s,sat} \approx \theta_{s,max}$) will not act in accordance with the exposure metric. However, S_{rx} behavior can also be observed when $\theta_{s,sat} < \theta_{s,max}$ if the adsorption equilibrium constant K_{ads} dictates that only partial surface coverage can be achieved at equilibrium with gas-phase X (here $\theta_s \approx \theta_{s,sat}$, but $\theta_{s,sat} < \theta_{s,max}$). Here, increasing $[X]_g$ will increase the surface coverage, leading to a faster overall rate of reaction. In this non-saturated S_{rx} case, the gas uptake is thus also sensitive to K_{ads}, which in turn depends on both $\alpha_{s,0}$ and τ_d. The lack of sensitivity to $[X]_g$ in the bulk diffusion limited cases, S_{bd} and B_{bd}, arises due to the rate-limitation that the diffusion of Y poses. This process is obviously not accelerated by an increase in trace gas concentration. Thus, S_{bd} behavior, which is entirely limited by diffusion of Y, shows no dependence on $[X]_g$. B_{bd} cases still respond to an increase in $[X]_g$ since the combined diffusion of X and Y is rate-limiting here. Thus, the sensitivity to $[X]_g$ will always be smaller than unity but higher than zero in a B_{bd} case.

ACPD
13, 983–1044, 2013

The sensitivity analysis also provided information on the expected response of each limiting case to changes in particle size. The data displayed in Table 4 for $S(r_p)$ show the influence of particle size on reactive half-life. Using Eq. 19 to interpret the sensitivity coefficients, these results show that the reactive half-life of systems which are limited by surface-related processes have an inverse dependence on particle size ($S(r_p) = -1$), systems which are limited by diffusion have an inverse-square dependence on particle size ($S(r_p) = -2$), and that the B_{rx} limiting case does not depend on particle size at all ($S(r_p) = 0$). We note that in bulk accommodation limited bulk reaction cases, B_α, the value of $S(r_p)$ is typically -1 if limitation arises due to inefficient accommodation of X on the surface, but may decrease to -2 when transport across the surface-bulk interface is the rate-limiting step. For a more detailed description of these two different B_α scenarios, see Appendix C.

Taken together, these characteristic behaviors and sensitivities can provide some insight into an experiment based only on the raw data. After making a preliminary assignment based on the decay shape of one data set, the sensitivities in Sect. 5.2 can be used together with additional experiments to confirm this assignment.

6 Case study: the oleic acid – ozone reaction system

The oleic acid – ozone reaction system is an extremely well studied system which has often been used as a benchmark for heterogeneous chemistry systems (see, e.g. the review of Zahardis and Petrucci, 2007), so it is reasonable that we apply the proposed classification scheme to this reaction system as a demonstration of its potential. We will begin with a brief overview of the current state of the art in modeling this system and then apply the classification scheme described above to previously published datasets. A comparison of these results with one another and with current work is difficult as each study uses a different nomenclature for the limiting cases which they consider. In the following discussion, the common symbol set proposed above will be used to facilitate comparisons between previous studies and this work. We stress that our fits to the

ACPD
13, 983–1044, 2013

experimental data are not equally likely to represent reality and we do not attempt to judge between them.

6.1 Background

In the past, limiting cases similar to those discussed here have been derived by both Smith et al. (2002) and Worsnop et al. (2002) for this reaction system, including resistor model-based analytical expressions for comparison to experimental results. In the era before depth-resolved computation of aerosol reaction was common, Smith et al. (2003) solved the partial differential equations of diffusion and reaction for this system to provide results resolved in time and depth but assumed the surface was saturated with respect to trace gas, a crucial assumption which disallows mass-transfer limited behavior and constrains all results to the reaction-diffusion regime.

The relationships between the limiting cases proposed here and those already published by Smith et al. (2002) (including revisions made in Hearn et al., 2005) as well as in Worsnop et al. (2002) are depicted in Table 5. The most striking differences between these cases and previous schemes is the underrepresentation of the mass-transfer regime: although Worsnop et al. offer a mass-transfer limited case, this only applies to a bulk reaction and is not necessarily a case limited by a single process. It thus represents a range of cases, all of which fall within our definition of the B^{mt} regime. Furthermore, we consider Case 2 of Worsnop et al. (2002), Case 1b of Smith et al. (2002) and Case 2 of Hearn et al. (2005) to be representations of the traditional reacto-diffusive case B^{rd}_{trad} within the reaction-diffusion regime, as all have a formulation which shows dependence on both the diffusion of X and the reaction rate coefficient and thus depend on more than one process to determine reactive uptake. To achieve B_{bd} behavior, the reacto-diffusive length of both X and Y must be exceedingly short.

ACPD
13, 983–1044, 2013

6.2 Ziemann (2005) data set

A well-supported kinetic parameter set for the oleic acid – ozone reaction system is provided by Pfrang et al. (2010), which used $\alpha_{s,0,X}$ as a fitting parameter to match model output to the experimental results of Ziemann (2005). In that study, the decreasing oleic acid content of 200 nm radius particles reacting with ozone at a molecular number density of $\sim 6.95 \times 10^{13}$ cm^{-3} in an environmental chamber was measured via Thermal Desorption Particle Beam Mass Spectrometry. The parameter set of Pfrang et al. is displayed in column 2 of Table 6 and will be referred to as base case 1 (bc1). The bc1 parameter set does not include a gas-phase diffusivity of ozone in air. Unless otherwise noted, we used $D_{g,X} = 0.14\,\mathrm{cm^2\,s^{-1}}$ (Massman, 1998). We begin our analysis by replicating the bc1 fit from Pfrang et al. (2010), resulting in very good agreement with the experimental data as shown in Fig. 6a. While this fit does not fall into a limiting case (see Sect. 4.2), it shows low values for SSR and BSR as well as $C_{g,X} \sim 1$, altogether indicative of the SB$^{\alpha}$ regime (see Fig. 3b). The classification parameters are given along with the input parameter values in Table 6 for two different points in reaction course.

Although the bc1 parameter set provides an excellent fit to the experimental results of Ziemann (2005), other studies have provided additional information which suggest that the oleic acid diffusion coefficient $D_{b,Y}$ is significantly higher than the original value of $1 \times 10^{-10}\,\mathrm{cm^2\,s^{-1}}$ (Shiraiwa et al., 2012a; Hearn et al., 2005) and that the desorption lifetime of ozone ($\tau_{d,X}$) is on the order of nanoseconds for polycyclic aromatic hydrocarbons (PAH, cf. Maranzana et al., 2005; Shiraiwa et al., 2011b) as well as for graphene (Lee et al., 2009). In a modified fit, bc1* (Table 6, column 3), we adopt the value proposed by Shiraiwa et al. (2012a), $1.9 \times 10^{-7}\,\mathrm{cm^2\,s^{-1}}$ and set $\tau_{d,X} = 1 \times 10^{-8}$ s. The change in $D_{b,Y}$ has only a small impact on the overall reaction speed, as diffusion of oleic acid is not involved in the limiting process (accommodation of ozone to the surface). The reduced surface desorption lifetime decreases the role of surface reac-

ACPD
13, 983–1044, 2013

tions so that the modified bc1* can be assigned B_α behavior. The fit is also displayed in Fig. 6a.

6.3 Lee and Chan (2007) data set

Lee and Chan (2007) used raman spectroscopy to measure the decay of oleic acid in 40–70 µm particles exposed to $\sim 6.36 \times 10^{12}$ cm^{-3} ozone in an electrodynamic balance. We apply a multi-parameter fit to this data set to find fits in reasonable proximity to the bc1* parameter set (Fits I–II, Table 6). Note that some values, including especially $\alpha_{s,0,X}$, are poorly constrained by experiment and were given large tolerances during the fitting process. The exact particle size was not reported in the original publication and particle size has thus been used as a fit parameter. We have varied the particle radius along with the non-bracketed parameters in Fits I (B_α) and II (B^{rd}) given in Table 6 to achieve a good fit to the decay shown in Fig. 6b, which is reproduced from the smaller of the two particles shown in Fig. 2 in Lee and Chan (2007).

The two fits shown here were calculated assuming a particle diameter of 40 µm for the smaller particle, which is within the size range estimated by Lee and Chan (2007). Due to the large particle size in this data set, the layer spacing scheme in KM-SUB had to be altered to achieve numerical convergence of the modeling result. From a total of 200 computed layers, 40 were chosen to form a narrowly resolved surface region. Each of these layers was attributed a depth of about 10 ozone monolayers (4 nm). The residual space was then equally distributed in depth among the 160 remaining layers. The consequences of using an insufficient number of layers, leading to non-resolved (step) gradients are briefly addressed in appendix C.

Both Fit I and Fit II are consistent with the observed decay and could only be distinguished from one another in fit quality in the final stages of the reaction, for which no data are available. However, Fit I directly matches the B_α assignment that was made for the data set of Ziemann (2005), while Fit II would only match a non-linear decay. Indeed, most previous observations of this system, which are summarized in the comprehensive review of Zahardis and Petrucci (2007), were generally non-linear in time.

ACPD
13, 983–1044, 2013

This is an example of the logical error which arises when limiting case behavior observed under one condition (small particles, high oxidant concentration) is assumed to apply elsewhere (very large particles, much lower oxidant concentration). We therefore continue with a more in-depth analysis of a data set measured with smaller particles at high oxidant concentration that shows a pronounced non-linearity and includes data to the very end of the reaction.

6.4 Hearn et al. (2005) data set

6.4.1 Analysis of a single data set

A second multi-parameter fit was applied to the aerosol Chemical Ionization Mass Spectrometric measurements in Hearn et al. (2005) (650 nm diameter oleic acid particles reacting with 2.76×10^{15} cm^{-3} ozone in an aerosol flow tube). As shown in Fig. 6c, the resulting fits exhibit B^{rd} regime and S_{rx} limiting case behavior, respectively. Although Fit III and Fit IV resemble the experimental data reasonably when viewed on a linear scale, the logarithmic representation of Fig. 6d shows that Fit III deviates marginally from the data after 2.0 s. This was already discussed by Hearn et al. for the traditional reacto-diffusive case B^{rd}_{trad}, which is a subset of the B^{rd} regime. The B^{rd}_{trad} case has a quadratic-like functional form in $N_Y(t)$ that is not able to fit the experimentally observed mono-exponential decay. In contrast to the ideal B^{rd}_{trad} case, Fit III does not show a true quadratic decay shape and lies significantly closer to the experimental data compared to the fit shown in Fig. 2 of Hearn et al. (2005). This improved fit arises because Fit III does not exactly match the B^{rd}_{trad} scenario and its kinetic behavior changes towards B_{rx} as the reaction proceeds.

A rather different picture of the internal structure of the aerosol particle is provided with Fit IV, showing an excellent fit to the experimental data in reasonable proximity to the original bc1 parameter set of Pfrang et al. (2010). This fully-saturated surface reaction is consistent with the conclusion of Hearn et al. (2005), who suggested that the reaction occurs exclusively on the particle surface as a result of a quasi-smectic

ACPD
13, 983–1044, 2013

structure of the uppermost oleic acid layer that is inpenetrable by ozone due to slow diffusion and fast reaction, respectively. We note that the surface reaction behavior in Fit IV is only achieved using a $\tau_{d,X}$ which is even longer than that of bc1, and may not be within the range of acceptable values for $\tau_{d,X}$ for the oleic acid – ozone system. Such a value would be acceptable only if a long-lived intermediate was formed (as discussed in Shiraiwa et al. (2011b) for PAH + O_3).

6.4.2 Using additional data to constrain limiting behavior

Both Fit III and Fit IV are in reasonable agreement with the single experimental decay in Fig. 6. However, further experimental results of Hearn et al. with differently sized particles indicate that the initial reaction rate scales inversely with the particle radius ($S^n(r_p) = -1$), which is typical for systems that are limited by a surface-related process such as S_{rx}, B_α or B^{rd}_{trad} (see Table 4). S_{rx} behavior as shown by Fit IV is thus very likely to represent the overall behavior of this system. Unlike Fit IV, which was found to reasonably match the experimentally observed response to particle size ($S^n(r_p) = -0.99$), Fit III shows a nearly inverse root dependence on particle size ($S^n(r_p) = -0.51$).

In agreement with the original study of Hearn et al., we conclude that S_{rx} is the only single limiting case that fits the experimental observations of both decay shape and scaling of initial reaction rate with particle size. However, a behavior which mixes the characteristics of more than one limiting case might also fit the data well, even though the limiting cases which it most closely resembles would fail individually. The Fit III parameter set presented here follows this logic by mixing the behaviors of B^{rd}_{trad} and B_{rx} to adequately represent both the non-linear decay of N_Y as a function of time and the scaling of the initial decay rate with particle radius. Although the agreement of Fit III with the experimental $N_Y(t)$ and $S^n(r_p)$ is not as good as that of Fit IV, both are in reasonable proximity to experimentally measured values. This opens up another possibility for modeling of the oleic acid – ozone system that has yet to be proven by a well-fitting kinetic parameter set.

ACPD
13, 983–1044, 2013

6.5 Sensitivity profiles of displayed limiting cases

As discussed in Sect. 4.3, we recommend sensitivity analysis to confirm that the numerical criteria chosen result in distinct and well-behaved limiting cases. Figure 7 shows the sensitivity profiles of the six parameter sets found for the oleic acid – ozone system in the previous section. In each case, the assignment is supported by the sensitivity analysis. Sensitivity coefficients are given at 10 % reaction course as this will reduce the potential influence of reaction products and avoids the initial, highly transient behavior which is expected as the surface and first bulk layers come into equilibrium with the gas phase. In general, sensitivity coefficients were not observed to vary significantly over time once a quasi-stationary state of transport and reaction is reached. In the event that behavior is not consistent throughout the reaction, a change in regime or limiting case behavior can be detected by a change in classification parameters and the sensitivity coefficients follow accordingly. For example, classification parameters for Fit III (Table 6) show an increase in mixing parameter BMP_{XY} over time, indicating a smooth transition from B^{rd} regime towards B_{rx} limiting case behavior. This is accompanied by a decrease in sensitivity towards the bulk diffusion coefficient $D_{b,X}$ from $S^n(D_{b,X}) = 0.22$ at 10 % reaction course to 0.16 at 50 % reaction course and 0.04 at 90 % reaction course.

The interpretation of the fits to Ziemann data, panels a and b of Fig. 7 is relatively straightforward. As expected from Table 3, these fits are only sensitive to the $\alpha_{s,0,X}$ parameter. Indeed, in panel a, only $\alpha_{s,0,X}$ is indicated as a direct control on the result of the calculation, in accordance with the accommodation regime (SB^{α}). In panel b, the sensitivity to $\alpha_{s,0,X}$ remains high while some minor dependence on parameters related to bulk reaction ($H_{cp,X}$, k_{BR}, $D_{b,X}$) is observed, both in agreement with the assignment as B_{α}.

Panels c and d show sensitivity analyses of fits to the Lee and Chan (2007) data and reveal very typical behavior for the B_{α} case and the B^{rd} regime, respectively. While Fit I in panel c is completely governed by the $\alpha_{s,0,X}$ parameter, Fit II in panel d shows

ACPD
13, 983–1044, 2013

the traditional reacto-diffusive behavior with a balanced sensitivity towards the reaction and diffusion process. In both cases, the large particle radius leads to a slight influence of gas-phase diffusion as indicated by sensitivity to $D_{g,X}$.

The interpretation of the fits to Hearn et al. (2005) data, panels e and f of Fig. 7 also confirms our assignments. In panel e, the parameters indicate a mixture of bulk reaction and bulk diffusion limiting cases (B^{rd} regime). Unlike Fit II in panel d, this case does not coincide with the traditional B^{rd}_{trad} case, as it shows a slight predominance towards reaction limitation and thus B_{rx} behavior. This example demonstrates the breadth of possible behaviors for cases that do not fall into a distinct limiting case but rather exhibit regime behavior. In panel f, only the surface reaction rate coefficient is influential, and thus S_{rx} behavior was correctly assigned.

In interpreting these sensitivity analyses, a low sensitivity does not necessarily mean that a process related to that parameter is unimportant, only that modest changes in that parameter do not have a strong influence on the model result. This could be the case if a parameter is obviated (e.g. the Henry's law constant in a system which reacts exclusively at the surface, in which case it could take on any value) or if a process is saturated (e.g. the reaction rate coefficient in an accommodation limited case, for which modest changes in k_{BR} would not matter as the reaction would remain "fast" compared to the accommodation process). Overall, the simple 9 : 1 numerical criteria proposed in Sect. 4.2 were sufficient for this system, but should be revisited for each new chemical system to ensure that limiting cases and regimes are well-behaved (that is, influenced by only one or two processes respectively).

7 Conclusions

The development of depth-resolved models for aerosol chemistry has prompted the more sophisticated, systematic classification of the kinetic behavior of aerosol particles proposed here. The set of limiting cases and associated symbols proposed above should allow a more complete and more intuitive discussion of aerosol particle be-

ACPD
13, 983–1044, 2013

havior, especially in systems which exhibit stiff coupling of physical and/or chemical processes. In particular, the more complete treatment of mass-transfer limitation presented in this study not only allows for analysis of such systems but may also assist in interpreting and reconciling previous studies.

Limiting case or kinetic regime assignments facilitate the interpretation of experimental data since, in principle, only the rate limiting process(es) have to be considered when calculating or analyzing reactive uptake. During an experimental study, results can be compared to the characteristic behaviors described in Sect. 5 which may provide insight into the kinetic behavior of aerosol particles. If the experimental results match a profile of a limiting case, the predicted sensitivity of the assigned case to experimental conditions may be useful in guiding follow-up experiments.

As outlined above, a single chemical reaction system can exhibit different kinetic behaviors depending on reaction conditions such as concentration levels and particle sizes. The classification scheme proposed here provides a means of characterizing a specific reaction system under specific conditions, but the underlying parameters which drive the physical and chemical behavior remain the most valuable information which models can extract from experimental data. This is particularly important for the extrapolation of laboratory results to atmospherically relevant conditions, a task which demands a well-constrained parameter set to provide reliable results. Therefore, we emphasize the need for experiments at different time scales, particle sizes and reactant concentrations, to provide enough constraints for accurate determination of fundamental kinetic parameters. In light of the breakdown of the exposure metric (oxidant concentration × time) for some aerosol behaviors, we recommend that studies which use the exposure metric should also provide independent concentration and time data for future reanalysis.

Multi-parameter fitting of three different datasets for the benchmark system of oleic acid reacting with ozone has shown that the available data can be represented by different sets of kinetic parameters that do not correspond to a single kinetic behavior

ACPD
13, 983–1044, 2013

(regime or limiting case). Using only one data set at a time for the fitting of several kinetic parameters resulted in an under-determined system.

We conclude that for a well-constrained kinetic parameter set, several data sets should be taken into account simultaneously to provide a sufficiently broad set of constraints for the fitting result. These sets must include a wide range of experimental conditions, since non-limiting parameters are only poorly constrained by experimental data. Multi-parameter fitting to multiple data sets for extraction of kinetic parameters would therefore be of general importance for modeling of multiphase chemistry, but requires a significantly higher technical effort. The prospects and challenges of multi-dimensional fitting to elucidate the kinetic parameters of aerosol reaction systems will thus be addressed in detail in a follow-up study, building on the classification framework provided here.

Appendix A

List of symbols and abbreviations

See Table A1.

Appendix B

Additional regimes

In addition to the reaction-diffusion and mass-transfer regimes used throughout this work, there are many other combinations of limiting cases to form regimes which are possible. Sorting by mixing parameter MP leads to the distinction in Fig. S1a, the diffusion regime and the reaction-accommodation regime. This separation is less common than that shown in Fig. 3a for analysis of chemical reactivity. The typical example of a system in the reaction-accommodation regime arises when a particle is well-mixed

ACPD
13, 983–1044, 2013

and neither saturated nor starved on trace gas X, SSR and/or BSR ≈ 0.5, meaning that reaction and accommodation occur on similar time scales and are thus closely coupled. Another possibility is shown in Fig. A1b, in which the separation is made between chemical rate limitation ("reaction regime") and all other possibilities ("mass-transport regime"). We view the mass-transport regime (not to be confused with the mass-transfer regime SB^{mt}) in Fig. A1b as too broad to be useful, as systems lying in this regime may encompass every limitation on chemical reaction rate except the actual rate coefficient.

Appendix C

Degeneracy in low diffusivity cases in instances where $BMP_X = 0$ and $BMP_Y = 1$

As already described in Sect. 2.2, the reaction-diffusion regime encompasses all cases limited by reaction and/or diffusion and the traditional reacto-diffusive case within this regime, B^{rd}_{trad}, occurs when STLR≈ 0, BSR≈ 1, BMP_X ≈0 and $BMP_Y \approx 1$. In this situation, the surface and first subsurface bulk layer are saturated with X and the short reacto-diffusive length of X limits the reaction volume and thus reactive uptake. Although B^{rd}_{trad} cases have very strong gradients in X, they do not belong to the B_{bd} limiting case because the reaction and the diffusion of X are inherently coupled, and a limiting case is defined in this paper as being limited by only one process (Sect. 2.1).

In addition to the B^{rd}_{trad} case, another behavior can also be observed when $BMP_X \approx 0$, $BMP_Y \approx 1$, SSR ≈ 1, but BSR ≈ 0. Here, the surface is saturated with X but the transfer from surface to bulk is inefficient compared to reaction in the bulk. Since BSR ≈ 0 in this situation, this case is correctly assigned as a B_α case, and has a behavior which is consistent with the archetypal B_α case described in Sect. 5.1. We will distinguish this surface to bulk transfer limited case from the gas to surface limited case by referring to each as $B_{\alpha,s\rightarrow b}$ and $B_{\alpha,g\rightarrow s}$, respectively.

ACPD
13, 983–1044, 2013

Typically, the values of SSR and BSR are expected to be similar (for an overview of the relationship between SSR and BSR for different limiting cases and regimes, see Table S3). As suggested by the name "surface to bulk transfer limited", a discrepancy between SSR and BSR arises in the $B_{\alpha,s\rightarrow b}$ case. This situation depends crucially on the layer spacing in the model. Such a discrepancy between SSR and BSR could arise when the reacto-diffusive length is so short that it falls below layer spacing, which is often constrained to be one molecular length (e.g. a monolayer of Y) or larger. In such a situation, the assumption of internally well-mixed model layers is violated and the quasi-static surface layer acts as a diffusional bottleneck that has to be surpassed before bulk reaction can occur. This effectively decouples the reaction and diffusion process. However, the treatment of competing reaction and diffusion at the molecular level might not be well-represented by the kinetic model applied here and thus lies beyond the scope of this paper.

A more intuitive example for a $B_{\alpha,s\rightarrow b}$ case is a particle that is coated by an inert and only slowly penetrable shell such as a monolayer of saturated fatty acids (Rouvière and Ammann, 2010).

Supplementary material related to this article is available online at: http://www.atmos-chem-phys-discuss.net/13/983/2013/acpd-13-983-2013-supplement.pdf.

Acknowledgements. TB acknowledges support from the European Union Lifelong Learning Programme. AJH was supported by the United States National Science Foundation under award no. IRFP 1006117 and by ETH Zürich. MA appreciated support by the Swiss National Science Foundation (grant no. 130175). MS is supported by the Japan Society for the Promotion of Science (JSPS) Postdoctoral Fellowship for Research Abroad and the EU project PEGASOS (grant no. 265148). Any opinions, findings, and conclusions or recommendations expressed in this material are those of the authors and do not necessarily reflect the views of the US National Science Foundation. TB and AJH thank U. Krieger and T. Peter for their sup-

ACPD
13, 983–1044, 2013

port and for many useful conversations. TB would like to thank P. Ziemann, G. Smith, C. Chan and A. Lee for providing original data sets.

References

Abbatt, J. P. D., Lee, A. K. Y., and Thornton, J. A.: Quantifying trace gas uptake to tropospheric aerosol: recent advances and remaining challenges, Chem. Soc. Rev., 41, 6555–6581, doi:10.1039/C2CS35052A, 2012. 987, 999

Ammann, M., Rossler, E., Strekowski, R., and George, C.: Nitrogen dioxide multiphase chemistry: uptake kinetics on aqueous solutions containing phenolic compounds, Phys. Chem. Chem. Phys., 7, 2513–2518, doi:10.1039/B501808K, 2005. 999

Bates, D. V.: Detection of chronic respiratory bronchiolitis in oxidant-exposed populations: analogy to tobacco smoke exposure, Environ. Health Pers., 101, 217–218, avaiable at: http://www.ncbi.nlm.nih.gov/pmc/articles/PMC1519706/, 1993. 986

Behr, P., Morris, J. R., Antman, M. D., Ringeisen, B. R., Splan, J. R., and Nathanson, G. M.: Reaction and desorption of HCl and HBr following collisions with supercooled sulfuric acid, Geophys. Res. Lett., 28, 1961–1964, doi:10.1029/2000GL012716, 2001. 1000

Behr, P., Scharfenort, U., Ataya, K., and Zellner, R.: Dynamics and mass accommodation of HCl molecules on sulfuric acid-water surfaces, Phys. Chem. Chem. Phys., 11, 8048–8055, doi:10.1039/B904629A, 2009. 1000

Cariboni, J., Gatelli, D., Liska, R., and Saltelli, A.: The role of sensitivity analysis in ecological modelling, Ecol. Model., 203, 167–182, doi:10.1016/j.ecolmodel.2005.10.045, 2007. 987

Crowley, J. N., Ammann, M., Cox, R. A., Hynes, R. G., Jenkin, M. E., Mellouki, A., Rossi, M. J., Troe, J., and Wallington, T. J.: Evaluated kinetic and photochemical data for atmospheric chemistry: Volume V – heterogeneous reactions on solid substrates, Atmos. Chem. Phys., 10, 9059–9223, doi:10.5194/acp-10-9059-2010, 2010. 986

Danckwerts, P. V.: Absorption by simultaneous diffusion and chemical reaction into particles of various shapes and into falling drops, Trans. Faraday Soc., 47, 1014–1023, doi:10.1039/TF9514701014, 1951. 990

Davidovits, P., Hu, J. H., Worsnop, D. R., Zahniser, M. S., and Kolb, C. E.: Entry of gas molecules into liquids, Faraday Discuss., 100, 65–81, doi:10.1039/FD9950000065, 1995. 990

Davidovits, P., Kolb, C. E., Williams, L. R., Jayne, J. T., and Worsnop, D. R.: Mass accommodation and chemical reactions at gas–liquid interfaces, Chem. Rev., 106, 1323–1354, doi:10.1021/cr040366k, 2006. 990

Deiber, G., George, Ch., Le Calvé, S., Schweitzer, F., and Mirabel, Ph.: Uptake study of $ClONO_2$ and $BrONO_2$ by Halide containing droplets, Atmos. Chem. Phys., 4, 1291–1299, doi:10.5194/acp-4-1291-2004, 2004. 1004

Donaldson, D. J., Ravishankara, A. R., and Hanson, D. R.: Detailed Study of HOCl + HCl → $C_l2 + H_2O$ in Sulfuric Acid, J. Phys. Chem. A, 101, 4717–4725, doi:10.1021/jp9633153, 1997. 1003

Dunker, A. M.: The decoupled direct method for calculating sensitivity coefficients in chemical kinetics, J. Chem. Phys., 81, 2385–2393, doi:10.1063/1.447938, 1984. 987

George, I. J., Matthews, P. S., Brooks, B., Goddard, A., Whalley, L. K., Baeza-Romero, M. T., and Heard, D. E.: Heterogeneous Uptake of HO_2 Radicals onto Atmospheric Aerosols, abstract A43D-0186, presented at Fall Meeting, AGU, San Francisco, Calif., 5–9 Dec., 2011. 999

Hanson, D. R. and Lovejoy, E. R.: Heterogeneous reactions in liquid sulfuric acid: HOCl + HCl as a model system, J. Phys. Chem.-US, 100, 6397–6405, doi:10.1021/jp953250o, 1996. 1003

Hanson, D. R., Ravishankara, A. R., and Solomon, S.: Heterogeneous reactions in sulfuric acid aerosols: a framework for model calculations, J. Geophys. Res., 99, 3615–3629, doi:10.1029/93JD02932, 1994. 986, 988, 990

Hearn, J. D., Lovett, A. J., and Smith, G. D.: Ozonolysis of oleic acid particles: evidence for a surface reaction and secondary reactions involving Criegee intermediates, Phys. Chem. Chem. Phys., 7, 501–511, doi:10.1039/B414472D, 2005. 1003, 1011, 1012, 1014, 1015, 1017, 1035, 1043, 1044

Hu, J. H., Shi, Q., Davidovits, P., Worsnop, D. R., Zahniser, M. S., and Kolb, C. E.: Reactive uptake of Cl_2(g) and Br_2(g) by aqueous surfaces as a function of Br^- and I^- ion concentration: the effect of chemical reaction at the interface, J. Phys. Chem., 99, 8768–8776, doi:10.1021/j100021a050, 1995. 1000

IPCC: Climate Change 2007: The Physical Science Basis, Contribution of Working Group I to the Fourth Assessment Report of the Intergovernmental Panel on Climate Change, Cambridge University Press, Cambridge, United Kingdom and New York, NY, USA, 2007. 986

Jakab, G. J., Spannhake, E. W., Canning, B. J., Kleeberger, S. R., and Gilmour, M. I.: The effects of ozone on immune function, Environ. Health Pers., 103, 77–89, available at: http://www.ncbi.nlm.nih.gov/pmc/articles/PMC1518840/, 1995. 986

Kanakidou, M., Seinfeld, J. H., Pandis, S. N., Barnes, I., Dentener, F. J., Facchini, M. C., Van Dingenen, R., Ervens, B., Nenes, A., Nielsen, C. J., Swietlicki, E., Putaud, J. P., Balkanski, Y., Fuzzi, S., Horth, J., Moortgat, G. K., Winterhalter, R., Myhre, C. E. L., Tsigaridis, K., Vignati, E., Stephanou, E. G., and Wilson, J.: Organic aerosol and global climate modelling: a review, Atmos. Chem. Phys., 5, 1053–1123, doi:10.5194/acp-5-1053-2005, 2005. 986

Knipping, E. M. and Dabdub, D.: Modeling Cl_2 formation from aqueous NaCl particles: Evidence for interfacial reactions and importance of Cl_2 decomposition in alkaline solution, J. Geophys. Res., 107, 4360, doi:10.1029/2001JD000867, 2002. 1000

Knipping, E. M., Lakin, M. J., Foster, K. L., Jungwirth, P., Tobias, D. J., Gerber, R. B., Dabdub, D., and Finlayson-Pitts, B. J.: Experiments and simulations of ion-enhanced interfacial chemistry on aqueous NaCl aerosols, Science, 288, 301–306, doi:10.1126/science.288.5464.301, 2000. 1000

Kolb, C., Worsnop, D., Jayne, J., and Davidovits, P.: Comment on mathematical models of the uptake of $ClONO_2$ and other gases by atmospheric aerosols, J. Aerosol Sci., 29, 893–897, doi:10.1016/S0021-8502(97)10022-2, 1998. 990

Kolb, C. E., Cox, R. A., Abbatt, J. P. D., Ammann, M., Davis, E. J., Donaldson, D. J., Garrett, B. C., George, C., Griffiths, P. T., Hanson, D. R., Kulmala, M., McFiggans, G., Pöschl, U., Riipinen, I., Rossi, M. J., Rudich, Y., Wagner, P. E., Winkler, P. M., Worsnop, D. R., and O' Dowd, C. D.: An overview of current issues in the uptake of atmospheric trace gases by aerosols and clouds, Atmos. Chem. Phys., 10, 10561–10605, doi:10.5194/acp-10-10561-2010, 2010. 986, 990

Koop, T., Bookhold, J., Shiraiwa, M., and Pöschl, U.: Glass transition and phase state of organic compounds: dependency on molecular properties and implications for secondary organic aerosols in the atmosphere, Phys. Chem. Chem. Phys., 13, 19238–19255, doi:10.1039/C1CP22617G, 2011. 1000

Laskin, A., Gaspar, D. J., Wang, W., Hunt, S. W., Cowin, J. P., Colson, S. D., and Finlayson-Pitts, B. J.: Reactions at interfaces as a source of sulfate formation in sea-salt particles, Science, 301, 340–344, doi:10.1126/science.1085374, 2003. 1000

ACPD
13, 983–1044, 2013

Lee, A. K. and Chan, C. K.: Single particle Raman spectroscopy for investigating atmospheric heterogeneous reactions of organic aerosols, Atmos. Environ., 41, 4611–4621, doi:10.1016/j.atmosenv.2007.03.040, 2007. 1003, 1013, 1016, 1035, 1043, 1044

Lee, G., Lee, B., Kim, J., and Cho, K.: Ozone adsorption on graphene: ab initio study and experimental validation, J. Phys. Chem. C., 113, 14225–14229, doi:10.1021/jp904321n, 2009. 1012

Maranzana, A., Serra, G., Giordana, A., Tonachini, G., Barco, G., and Causà, M.: Ozone interaction with polycyclic aromatic hydrocarbons and soot in atmospheric processes: theoretical density functional study by molecular and periodic methodologies, J. Phys. Chem. A, 109, 10929–10939, doi:10.1021/jp053672q, 2005. 1012

Martien, P. T. and Harley, R. A.: Adjoint sensitivity analysis for a three-dimensional photochemical model: application to Southern California, Environ. Sci. Technol., 40, 4200–4210, doi:10.1021/es051026z, 2006. 987

Massman, W.: A review of the molecular diffusivities of H_2O, CO_2, CH_4, CO, O_3, SO_2, NH_3, N_2O, NO, and NO_2 in air, O_2 and N_2 near STP, Atmos. Environ., 32, 1111–1127, doi:10.1016/S1352-2310(97)00391-9, 1998. 1012

McConnell, R., Berhane, K., Gilliland, F., London, S. J., Islam, T., Gauderman, W. J., Avol, E., Margolis, H. G., and Peters, J. M.: Asthma in exercising children exposed to ozone: a cohort study, Lancet, 359, 386–391, doi:10.1016/S0140-6736(02)07597-9, 2002. 986

Mikhailov, E., Vlasenko, S., Martin, S. T., Koop, T., and Pöschl, U.: Amorphous and crystalline aerosol particles interacting with water vapor: conceptual framework and experimental evidence for restructuring, phase transitions and kinetic limitations, Atmos. Chem. Phys., 9, 9491–9522, doi:10.5194/acp-9-9491-2009, 2009. 1000

Morris, J. R., Behr, P., Antman, M. D., Ringeisen, B. R., Splan, J., and Nathanson, G. M.: Molecular beam scattering from supercooled sulfuric acid: collisions of HCl, HBr, and HNO_3 with 70 wt D_2SO_4, J. Phys. Chem. A, 104, 6738–6751, doi:10.1021/jp000105o, 2000. 1000

Morris, M.: Factorial sampling plans for preliminary computational experiments, Technometrics, 33, 161–174, available at: http://www.jstor.org/stable/10.2307/1269043, 1991. 1004, 1044

Nel, A.: Air pollution-related illness: effects of particles, Science, 308, 804–806, doi:10.1126/science.1108752, 2005. 986

Oldridge, N. W. and Abbatt, J. P. D.: Formation of gas-phase bromine from interaction of ozone with frozen and liquid NaCl/NaBr solutions: quantitative separation of surficial chemistry from bulk-phase reaction, J. Phys. Chem. A, 115, 2590–2598, doi:10.1021/jp200074u, 2011. 1001

ACPD
13, 983–1044, 2013

Pfrang, C., Shiraiwa, M., and Pöschl, U.: Coupling aerosol surface and bulk chemistry with a kinetic double layer model (K2-SUB): oxidation of oleic acid by ozone, Atmos. Chem. Phys., 10, 4537–4557, doi:10.5194/acp-10-4537-2010, 2010. 1012, 1014, 1035

Pfrang, C., Shiraiwa, M., and Pöschl, U.: Chemical ageing and transformation of diffusivity in semi-solid multi-component organic aerosol particles, Atmos. Chem. Phys., 11, 7343–7354, doi:10.5194/acp-11-7343-2011, 2011. 1001

Pöschl, U., Rudich, Y., and Ammann, M.: Kinetic model framework for aerosol and cloud surface chemistry and gas-particle interactions – Part 1: General equations, parameters, and terminology, Atmos. Chem. Phys., 7, 5989–6023, doi:10.5194/acp-7-5989-2007, 2007. 988, 990, 993, 998, 1002, 1038

Ravishankara, A. R.: Heterogeneous and multiphase chemistry in the troposphere, Science, 276, 1058–1065, doi:10.1126/science.276.5315.1058, 1997. 990

Ravishankara, A. R. and Longfellow, C. A.: Reactions on tropospheric condensed matter Plenary Lecture, Phys. Chem. Chem. Phys., 1, 5433–5441, doi:10.1039/A905660B, 1999. 990

Renbaum, L. H. and Smith, G. D.: Artifacts in measuring aerosol uptake kinetics: the roles of time, concentration and adsorption, Atmos. Chem. Phys., 11, 6881–6893, doi:10.5194/acp-11-6881-2011, 2011. 1006, 1007

Rouvière, A. and Ammann, M.: The effect of fatty acid surfactants on the uptake of ozone to aqueous halogenide particles, Atmos. Chem. Phys., 10, 11489–11500, doi:10.5194/acp-10-11489-2010, 2010. 1021

Rouvière, A., Sosedova, Y., and Ammann, M.: Uptake of ozone to deliquesced KI and mixed KI/NaCl aerosol particles, J. Phys. Chem. A, 114, 7085–7093, doi:10.1021/jp103257d, 2010. 1004

Saltelli, A., Ratto, M., Andres, T., Campolongo, F., Cariboni, J., Gatelli, D., Saisana, M., and Tarantola, S.: Global sensitivity analysis: the primer, Wiley Online Library, doi:10.1002/9780470725184.fmatter, last access: 15 November 2011, 2008. 987, 1004, 1005, 1044

Schwartz, S.: Mass-Transport Considerations Pertinent to Aqueous Phase Reactions of Gases in Liquid-Water Clouds, NATO ASI Series, vol. G6, Springer Verlag, Heidelberg, Germany, chemistry of multiphase atmospheric systems, 1986. 990

Schwartz, S. and Freiberg, J. E.: Mass-transport limitation to the rate of reaction of gases in liquid droplets: application to oxidation of SO_2 in aqueous solutions, Atmos. Environ., 15, 1129–1144, doi:10.1016/0004-6981(81)90303-6, 1981. 988

ACPD
13, 983–1044, 2013

Seinfeld, J. H. and Pandis, S. N.: Atmospheric Chemistry and Physics: From Air Pollution to Climate Change, Wiley, New York, 2006. 999

Shaka', H., Robertson, W. H., and Finlayson-Pitts, B. J.: A new approach to studying aqueous reactions using diffuse reflectance infrared Fourier transform spectrometry: application to the uptake and oxidation of SO2 on OH-processed model sea salt aerosol, Phys. Chem. Chem. Phys., 9, 1980–1990, doi:10.1039/B612624C, 2007. 1000

Shiraiwa, M., Garland, R. M., and Pöschl, U.: Kinetic double-layer model of aerosol surface chemistry and gas-particle interactions (K2-SURF): Degradation of polycyclic aromatic hydrocarbons exposed to O_3, NO_2, H_2O, OH and NO_3, Atmos. Chem. Phys., 9, 9571–9586, doi:10.5194/acp-9-9571-2009, 2009. 999

Shiraiwa, M., Pfrang, C., and Pöschl, U.: Kinetic multi-layer model of aerosol surface and bulk chemistry (KM-SUB): the influence of interfacial transport and bulk diffusion on the oxidation of oleic acid by ozone, Atmos. Chem. Phys., 10, 3673–3691, doi:10.5194/acp-10-3673-2010, 2010. 987, 1002, 1038

Shiraiwa, M., Ammann, M., Koop, T., and Pöschl, U.: Gas uptake and chemical aging of semisolid organic aerosol particles, P. Natl. Acad. Sci. USA, 108, 11003–11008, doi:10.1073/pnas.1103045108, 2011a. 987, 1000

Shiraiwa, M., Sosedova, Y., Rouvière, A., Yang, H., Zhang, Y., Abbatt, J. P. D., Ammann, M., and Pöschl, U.: The role of long-lived reactive oxygen intermediates in the reaction of ozone with aerosol particles, Nat. Chem., 3, 291–295, doi:10.1038/nchem.988, 2011b. 1012, 1015

Shiraiwa, M., Pfrang, C., Koop, T., and Pöschl, U.: Kinetic multi-layer model of gas-particle interactions in aerosols and clouds (KM-GAP): linking condensation, evaporation and chemical reactions of organics, oxidants and water, Atmos. Chem. Phys., 12, 2777–2794, doi:10.5194/acp-12-2777-2012, 2012. 1012

Shiraiwa, M., Pöschl, U., and Knopf, D. A.: Multiphase chemical kinetics of NO_3 radicals reacting with organic aerosol components from biomass burning, Environ. Sci. Technol., 46, 6630–6636, doi:10.1021/es300677a, 2012b. 1000

Shiraiwa, M., Selzle, K., Yang, H., Sosedova, Y., Ammann, M., and Pöschl, U.: Multiphase chemical kinetics of the nitration of aerosolized protein by ozone and nitrogen dioxide, Environ. Sci. Technol., 46, 6672–6680, doi:10.1021/es300871b, 2012c. 1000

Smith, G. D., Woods, E., DeForest, C. L., Baer, T., and Miller, R. E.: Reactive uptake of ozone by oleic acid aerosol particles: application of single-particle mass spectrometry to heteroge-

ACPD
13, 983–1044, 2013

neous reaction kinetics, J. Phys. Chem. A, 106, 8085–8095, doi:10.1021/jp020527t, 2002. 1011

Smith, G. D., Woods, E., Baer, T., and Miller, R. E.: Aerosol uptake described by numerical solution of the diffusion–reaction equations in the particle, J. Phys. Chem. A, 107, 9582–9587, doi:10.1021/jp021843a, 2003. 1011

Streets, D. G., Bond, T. C., Lee, T., and Jang, C.: On the future of carbonaceous aerosol emissions, J. Geophys. Res., 109, D24212, doi:10.1029/2004JD004902, 2004. 986

Tong, H.-J., Reid, J. P., Bones, D. L., Luo, B. P., and Krieger, U. K.: Measurements of the timescales for the mass transfer of water in glassy aerosol at low relative humidity and ambient temperature, Atmos. Chem. Phys., 11, 4739–4754, doi:10.5194/acp-11-4739-2011, 2011. 1000

Virtanen, A., Joutsensaari, J., Koop, T., Kannosto, J., Yli-Pirila, P., Leskinen, J., Makela, J. M., Holopainen, J. K., Pöschl, U., Kulmala, M., Worsnop, D. R., and Laaksonen, A.: An amorphous solid state of biogenic secondary organic aerosol particles, Nature, 467, 824–827, doi:10.1038/nature09455, 2010. 1000

Worsnop, D. R., Morris, J. W., Shi, Q., Davidovits, P., and Kolb, C. E.: A chemical kinetic model for reactive transformations of aerosol particles, Geophys. Res. Lett., 29, 1996, doi:10.1029/2002GL015542, 2002. 1011, 1034

Yu, H., Kaufman, Y. J., Chin, M., Feingold, G., Remer, L. A., Anderson, T. L., Balkanski, Y., Bellouin, N., Boucher, O., Christopher, S., DeCola, P., Kahn, R., Koch, D., Loeb, N., Reddy, M. S., Schulz, M., Takemura, T., and Zhou, M.: A review of measurement-based assessments of the aerosol direct radiative effect and forcing, Atmos. Chem. Phys., 6, 613–666, doi:10.5194/acp-6-613-2006, 2006. 986

Zahardis, J. and Petrucci, G. A.: The oleic acid-ozone heterogeneous reaction system: products, kinetics, secondary chemistry, and atmospheric implications of a model system – a review, Atmos. Chem. Phys., 7, 1237–1274, doi:10.5194/acp-7-1237-2007, 2007. 986, 1010, 1013

Ziemann, P. J.: Aerosol products, mechanisms, and kinetics of heterogeneous reactions of ozone with oleic acid in pure and mixed particles, Faraday Discuss., 130, 469–490, doi:10.1039/B417502F, 2005. 1003, 1012, 1013, 1016, 1035, 1044

Zobrist, B., Marcolli, C., Pedernera, D. A., and Koop, T.: Do atmospheric aerosols form glasses?, Atmos. Chem. Phys., 8, 5221–5244, doi:10.5194/acp-8-5221-2008, 2008. 1000

ACPD
13, 983–1044, 2013

Zobrist, B., Soonsin, V., Luo, B. P., Krieger, U. K., Marcolli, C., Peter, T., and Koop, T.: Ultra-slow water diffusion in aqueous sucrose glasses, Phys. Chem. Chem. Phys., 13, 3514–3526, doi:10.1039/C0CP01273D, 2011. 987, 1000

ACPD
13, 983–1044, 2013

Table 1. The principle regimes and limiting cases, defined in terms of two and three classification parameters respectively. The classification properties are the surface to total loss rate ratio (STLR), the saturation ratio(s) (SR) and the mixing parameter(s) (MP). When more than one expression for a classification property is possible (SR/MP), the expression is listed along with a rough criterion.

STLR	SR	Regime	MP	Limiting Case	Description
≈ 1	SSR ≈ 1	S^{rd}	$SMP_Y \approx 1$	S_{rx}	Surface reaction, limited by chemical reaction
			$SMP_Y \approx 0$	S_{bd}	Surface reaction limited by bulk diffusion of condensed reactant Y
≈ 1	SSR ≈ 0	S^{mt}	$C_{g,X} \approx 1$	S_α	Surface reaction limited by surface accommodation of X
			$C_{g,X} \approx 0$	S_{gd}	Surface reaction limited by gas-phase diffusion of X
≈ 0	BSR ≈ 1	B^{rd}	$BMP_{XY} \approx 1$	B_{rx}	Bulk reaction limited by chemical reaction rate
			$BMP_{XY} \approx 0$	B_{bd}	Bulk reaction limited by bulk diffusion of volatile reactant X and condensed reactant Y
≈ 0	BSR ≈ 0	B^{mt}	$C_{g,X} \approx 1$	B_α	Bulk reaction limited by bulk accommodation of X
			$C_{g,X} \approx 0$	B_{gd}	Bulk reaction limited by gas-phase diffusion of X

ACPD
13, 983–1044, 2013

Table 2. Kinetic input parameters in the KM-SUB representation of aerosol chemistry.

Parameter	Description	Units
k_{BR}	2nd order bulk reaction rate coefficient	$cm^3\,s^{-1}$
k_{SLR}	2nd order surface reaction rate coefficient	$cm^2\,s^{-1}$
$D_{b,X}$	Bulk diffusion coefficient of X in Y	$cm^2\,s^{-1}$
$D_{b,Y}$	Self-diffusion coefficient of Y	$cm^2\,s^{-1}$
$H_{cp,X}$	Henry's law solubility coefficient of X in Y	$mol\,cm^{-3}\,atm^{-1}$
$\tau_{d,X}$	Desorption lifetime of X	s
$\alpha_{s,0,X}$	Accommodation coefficient of X on a surface of bare Y	–
$D_{g,X}$	Gas-phase diffusion coefficient of X	$cm^2\,s^{-1}$

ACPD
13, 983–1044, 2013

Table 3. List of kinetic regimes and limiting cases and their respective controlling processes. Limiting cases are characterized by being controlled by one process, while systems in the regimes shown here are controlled by at most two processes. The parameters which influence the processes are given in a separate column and are defined in Table 2.

Limiting Processes	Parameters	Regime/Limiting Case		Limiting Process	Parameter(s)
Reaction and diffusion (surface)	k_{SLR}, $D_{b,Y}$, K_{ads}	S^{rd}	S_{rx} S_{bd}	Reaction at surface Bulk diffusion of Y	k_{SLR}, K^{a}_{ads} $D_{b,Y}$
Mass transfer of X to surface	$\alpha_{s,0,X}$, $D_{g,X}$	S^{mt}	S_{α} S_{gd}	Surface accommodation of X Gas-phase diffusion of X	$\alpha_{s,0,X}$ $D_{g,X}$
Reaction and diffusion (bulk)	k_{BR}, $D_{b,X}$, $D_{b,Y}$, H_X	B^{rd}	B_{rx} B^{rd}_{trad} B_{bd}	Reaction in bulk Equal parts reaction and diffusion Bulk diffusion of X and Y	k_{BR}, H_X k_{BR}, $D_{b,X}$, H_X $D_{b,X}$, H_X, $D_{b,Y}$
Mass transfer of X to bulk	$\alpha_{s,0,X}$, $D_{g,X}$, $D_{b,X}$, H_X	B^{mt}	B_{α} B_{gd}	Bulk accommodation of X Gas-phase diffusion of X	$\alpha_{s,0,X}$, $D_{b,X}$, H_X[b] $D_{g,X}$

[a]: K_{ads} is not a direct input parameter of the model, but inherently depends on $\tau_{d,X}$ and $\alpha_{s,0,X}$ as shown in Eq. (4).
[b]: These parameters altogether determine the bulk accommodation coefficient $\alpha_{b,X}$.

ACPD
13, 983–1044, 2013

Table 4. Scalability of limiting cases with respect to r_p and $[X]_g$ expressed by the normalized sensitivity coefficient of each archetypal case (see Eq. 19). Square brackets indicate the range of possible values.

Limiting Case	S^n_{rp}	$S^n_{[X]g}$
S_{rx}	−1	[0, 1]
S_{bd}	−2	0
S_{α}	−1	1
S_{gd}	−2	1
B_{rx}	0	1
B_{bd}	−2	[∼ 0, 1]
B_{α}	[−2, −1]	1
B_{gd}	−2	1
B^{rd}_{trad}, [a]	−1	1

[a]: Note that B^{rd}_{trad} is not a limiting case, but a distinct point in the reaction-diffusion regime.

ACPD
13, 983–1044, 2013

Table 5. Comparison of limiting cases proposed in this study to cases of the oleic acid – ozone system in previous studies. A "–" symbol indicates no relationship.

This study	Worsnop et al. (2002)	Smith et al. (2002)	Hearn et al. (2005)
S_{rx}	Case 4	Case 2	Case 3
S_{bd}	Case 5	–	Case 4
S_{α}	–	–	–
S_{gd}	–	–	–
B_{rx}	Case 3	Case 1a	Case 1
B_{trad}^{rd} [a]	Case 2	Case 1b	Case 2
B_{bd}	–	–	–
B_{α}	Case 1,[b]	–	–
B_{gd}		–	–

[a]: Note that B_{trad}^{rd} is not a limiting case, but a distinct point in the reaction-diffusion regime.

[b]: Case 1 of Worsnop et al. (2002) includes a range of cases inside the B^{mt} regime.

ACPD
13, 983–1044, 2013

Table 6. Kinetic parameter sets for KM-SUB that represent possible fits to experimental data provided by Ziemann (2005), Lee and Chan (2007) and Hearn et al. (2005). bc1, bc1* and Fit I are obtained by adjusting $\alpha_{s,0,X}$ while Fits II to IV are multi-parameter fits, obtained by least-squares fitting of modeled to experimental data. Even though Fits II and III do not exhibit limiting case behavior, they can still be assigned as a bulk reaction limited by reaction and diffusion (reacto-diffusion limitation). Values that were fixed during the fitting procedures are marked with square brackets.

Parameters	bc1,[a] Ziemann	bc1* Ziemann	Fit I Lee and Chan	Fit II Lee and Chan	Fit III Hearn	Fit IV (high $\tau_{d,X}$) Hearn
k_{BR} $\left(\frac{cm^3}{mol \cdot s}\right)$	$[1.70 \times 10^{-15}]$	$[1.70 \times 10^{-15}]$	$[1.70 \times 10^{-15}]$	2.52×10^{-16}	1.46×10^{-17}	2.10×10^{-16}
k_{SLR} $\left(\frac{cm^2}{mol \cdot s}\right)$	$[6.00 \times 10^{-12}]$	$[6.00 \times 10^{-12}]$	$[6.00 \times 10^{-12}]$	$[6.00 \times 10^{-12}]$	$[6.00 \times 10^{-12}]$	6.34×10^{-13}
$D_{b,X}$ $\left(\frac{cm^2}{s}\right)$	$[1.00 \times 10^{-5}]$	$[1.00 \times 10^{-5}]$	$[1.00 \times 10^{-5}]$	$[1.00 \times 10^{-5}]$	$[1.00 \times 10^{-5}]$	$[1.00 \times 10^{-5}]$
$D_{b,Y}$ $\left(\frac{cm^2}{s}\right)$	$[1.00 \times 10^{-10}]$	$[1.90 \times 10^{-7}]$	$[1.90 \times 10^{-7}]$	$[1.90 \times 10^{-7}]$	$[1.90 \times 10^{-7}]$	$[1.90 \times 10^{-7}]$
$H_{cp,X}$ $\left(\frac{mol}{cm^3 \cdot atm}\right)$	$[4.80 \times 10^{-4}]$	$[4.80 \times 10^{-4}]$	$[4.80 \times 10^{-4}]$	6.51×10^{-5}	2.30×10^{-3}	4.47×10^{-4}
$\tau_{d,X}$ (s)	$[1.00 \times 10^{-2}]$	$[1.00 \times 10^{-8}]$	$[1.00 \times 10^{-8}]$	$[1.00 \times 10^{-8}]$	$[1.00 \times 10^{-8}]$	5.23×10^{-1}[b]
$\alpha_{s,0,X}$ (–)	4.20×10^{-4}	4.61×10^{-4}	3.04×10^{-4}	4.18×10^{-2}	0.95×10^{-1}	5.48×10^{-2}
$D_{g,X}$ $\left(\frac{cm^2}{s}\right)$	$[1.4 \times 10^{-1}]$	$[1.4 \times 10^{-1}]$	$[1.4 \times 10^{-1}]$	$[1.4 \times 10^{-1}]$	$[1.4 \times 10^{-1}]$	$[1.4 \times 10^{-1}]$
10 % reaction course						
STLR	0.310	4.63×10^{-7}	3.52×10^{-7}	1.37×10^{-3}	2.06×10^{-4}	0.966
SR	0.082	0.079	0.031	0.905	0.951	0.996
MP	0.999	0.999	0.965	0.483	0.744	0.999
50 % reaction course						
STLR	0.259	3.61×10^{-7}	2.61×10^{-7}	9.00×10^{-4}	3.14×10^{-4}	0.964
SR	0.056	0.108	0.044	0.928	0.969	0.998
MP	0.999	0.999	0.966	0.482	0.7455	0.999
Regime/Limiting case	SB^{α}	B_{α},[c]	B_{α}	B^{rd}	B^{rd}	S_{rx}

[a] As provided by (Pfrang et al., 2010).
[b] This value implies formation of a long-lived intermediate.
[c] SR at 50 % reaction course is slightly outside the numerical criterion for this assignment.

ACPD
13, 983–1044, 2013

Table A1. List of symbols and abbreviations.

Symbol	Meaning	SI Unit
$\alpha_{b,X}$	bulk accommodation coefficient of X	
$\alpha_{s,X}$	surface accommodation coefficient of X	
$\alpha_{s,0,X}$	surface accommodation coefficient of X on an adsorbate-free surface	
γ_X	uptake coefficient of X (normalized by gas kinetic flux of surface collisions)	
$\gamma_{eff,X}$	effective uptake coefficient of X (normalized by average gas kinetic flux)	
δ_Y	effective molecular length of Y	m
$\theta_{s,X}$	surface coverage by X (sorption layer)	
$\theta_{s,max,X}$	maximum surface coverage by X (sorption layer)	
$\theta_{s,sat,X}$	saturation surface coverage by X (sorption layer)	
λ_i	kinetic input parameter *i*	
λ_X	mean free path of X in the gas phase	m
$\tau_{d,X}$	desorption lifetime of X	s
ω_X	mean thermal velocity of X	$m\,s^{-1}$
bc1	base case 1 input parameter set	
bc1*	modified base case 1 input parameter set	
BMP_X	mixing parameter for bulk diffusion of X (bulk reaction)	
BMP_Y	mixing parameter for bulk diffusion of Y (bulk reaction)	
BMP_{XY}	joint mixing parameter for bulk diffusion of X and Y (bulk reaction)	
BSR	bulk saturation ratio	
$C_{g,X}$	gas-phase diffusion correction factor for X and mixing parameter for gas phase X	
$D_{b,X}$	particle bulk diffusion coefficient of X	$m^2\,s^{-1}$
$D_{g,X}$	gas-phase diffusion coefficient of X	$m^2\,s^{-1}$
$H_{cp,X}$	Henry's law coefficient of X	$mol\,m^{-3}\,Pa^{-1}$
k_a	first-order adsorption rate coefficient of X	$m\,s^{-1}$
k_d	first-order desorption rate coefficient of X	s^{-1}
k_{BR}	second-order rate coefficient for bulk reactions	$m^3\,s^{-1}$
k_{SLR}	second-order rate coefficient for surface layer reactions	$m^2\,s^{-1}$
$K_{ads,X}$	adsorption equilibrium constant of X	m^3
$K_{sol,cc,X}$	dimensionless solubility or gas-particle partitioning coefficient of X	

ACPD
13, 983–1044, 2013

Table A1. Continued.

Symbol	Meaning	SI Unit
Kn_X	Knudsen number for X	
$l_{rd,X}$	reacto-diffusive length of X in Y	m
L_k	loss rate upon bulk reaction in layer k	s^{-1}
L_s	loss rate upon surface reaction	s^{-1}
SR	saturation ratio	
n	number of bulk layers in discretized representation of the particle	
N_Y	number of molecules of Y left in the aerosol particle	
r_p	particle radius	m
$S(\lambda_i)$	model sensitivity towards λ_i	
$S^n(\lambda_i)$	normalized model sensitivity towards λ_i	
SMP_Y	mixing parameter for bulk mixing of Y (surface reaction)	
SR	Saturation Ratio	
SSR	Surface Saturation Ratio	
STLR	Surface to Total Loss rate Ratio	
t	time	s
T	temperature	K
TLR	Total Loss Rate (of surface and bulk reaction)	s^{-1}
V_k	volume of layer k	m^3
X	trace gas species	
$[X]_{eff}$	effective bulk concentration of X experienced by reacting Y	m^{-3}
$[X]_g$	gas-phase number concentration of X	m^{-3}
$[X]_{gs}$	near-surface gas-phase number concentration of X	m^{-3}
$[X]_s$	surface number concentration of X (sorption layer)	m^{-2}
$[X]_{ss}$	subsurface number concentration of X (quasi-static surface layer)	m^{-2}
$[X]_{s,max}$	maximum surface number concentration of X (sorption layer)	m^{-2}
$[X]_{s,sat}$	saturation surface number concentration of X (sorption layer)	m^{-2}
$[X]_b$	particle bulk number concentration of X	m^{-3}
$[X]_{bk}$	number concentration of X in kth bulk layer	m^{-3}
$[X]_{b,sat}$	saturation particle bulk number concentration of X	m^{-3}
Y	bulk material species	
Y_{model}	model output	

ACPD
13, 983–1044, 2013

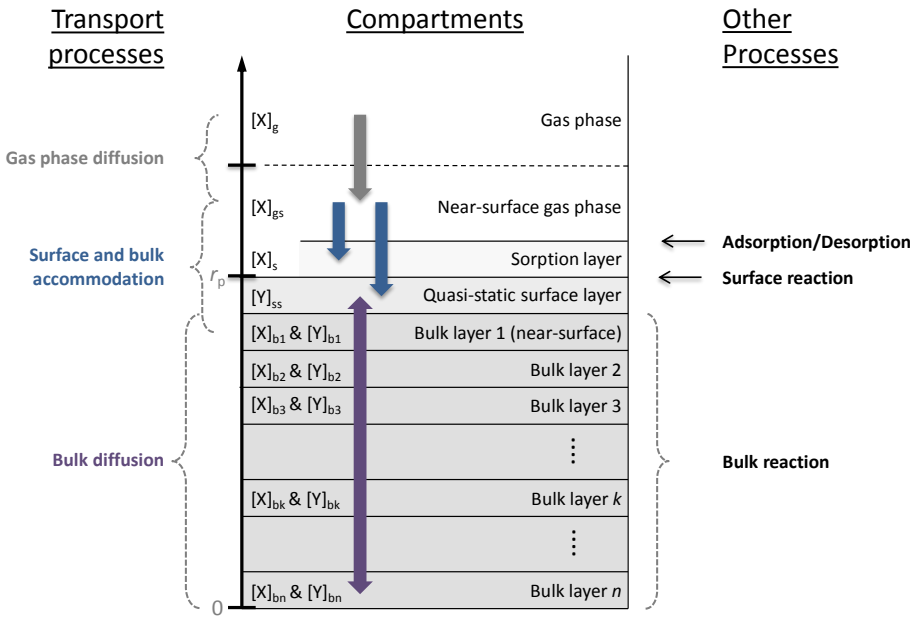

Fig. 1. Processes and compartments discussed in this paper (adapted from Shiraiwa et al., 2010), assuming a system which is either planar or spherically symmetric. Key processes are highlighted. Diffusion of gaseous trace gas X is assumed to influence the near surface gas-phase concentration $[X]_{gs}$ within one mean free path λ_x of the particle surface (r_p). Following Pöschl et al. (2007), surface accommodation denotes the mass flux of X from the near-surface gas phase to the particle surface, whereas bulk accommodation also includes the subsequent transport into the near-surface bulk. Surface reaction occurs between two layers, a sorption layer to which trace gas adsorbs, and the 2nd surface monolayer (quasi-static surface layer) consisting of bulk material Y. Reaction and diffusion can take place in *n* individually resolved bulk layers. All symbols are defined in Appendix A.

ACPD
13, 983–1044, 2013

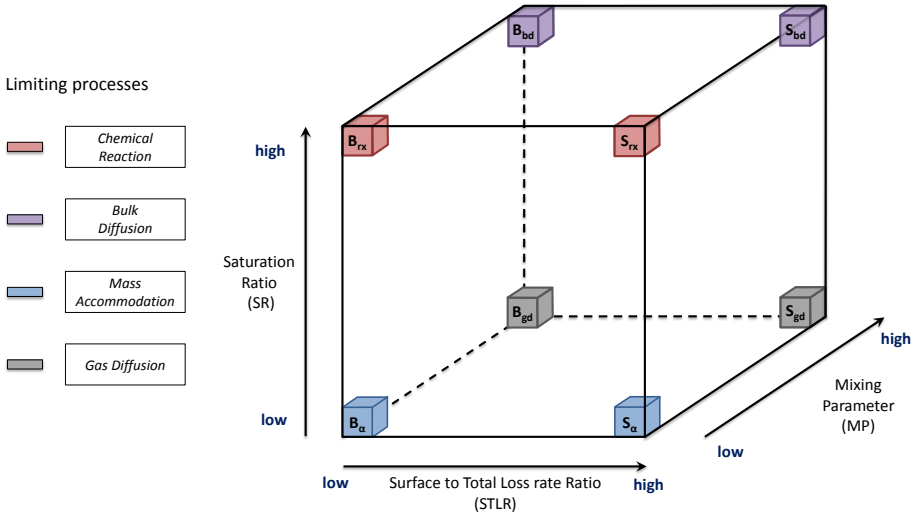

Fig. 2. The eight limiting cases can be depicted as the vertices of a cube in which every direction refers to a classification criterion (STLR, SR, MP). They are classified into four types of limiting behavior: limitation by chemical reaction, bulk diffusion, mass accommodation (including surface and bulk accommodation) and gas diffusion.

ACPD
13, 983–1044, 2013

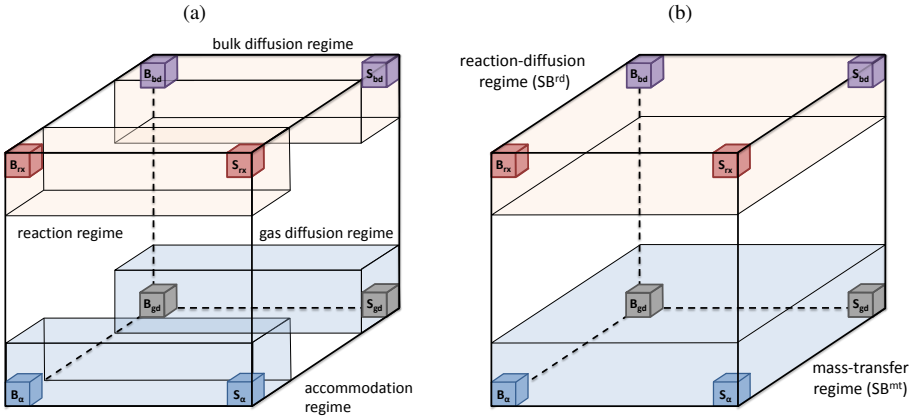

Fig. 3. Visualization of regimes as volumes of the cube in Fig. 2. **(a)** shows regimes resulting from the connection of each surface and bulk case. Regime names indicate the limiting process (the reaction regime is limited by reaction rate coefficients etc.). **(b)** shows a combination of the regimes in **(a)** in which the reaction and bulk diffusion regimes together form the reaction-diffusion regime and the accommodation and gas diffusion regimes together form the mass-transfer regime.

ACPD
13, 983–1044, 2013

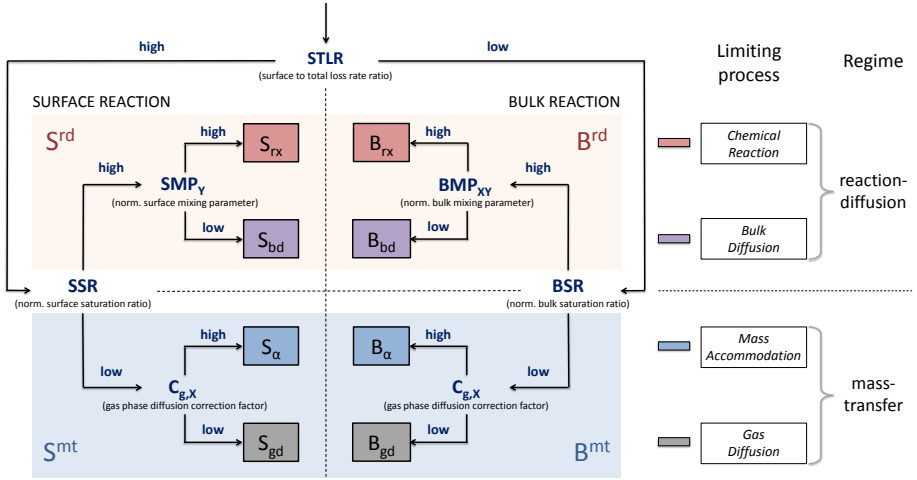

Fig. 4. Classification scheme for distinction of limiting cases. The decision process proceeds in three steps according to Sect. 2. Surface dominated cases (left half) and bulk dominated cases (right half) are distinguished in the first step by comparing the surface to the total loss rate (STLR). Reaction-diffusion systems (top half) and mass-transfer limited systems (bottom half) are distinguished in the second step by evaluating the saturation ratio (SR). In the last step mixing of the components is considered. Note that even though the scheme appears to be symmetric for surface and bulk reaction systems, the classification parameters differ between the left and the right side of the diagram in the second and third decision step. The reaction-diffusion and mass-transfer regimes are indicated by large shaded boxes and the respective regime symbols are given in their outward corners.

ACPD
13, 983–1044, 2013

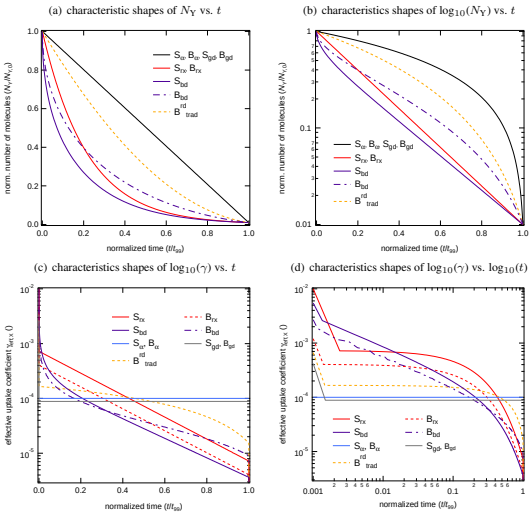

Fig. 5. Normalized representation of the decay shapes of the total amount of Y (N_Y) for all limiting cases established in this study. **(a)** reveals a linear decay for 4 different limiting cases, indicating a zeroth-order type process for all these scenarios. **(b)** shows a logarithmic version of **(a)** in which the B_{rx} and S_{rx} cases appear linear and can therefore be classified as mono-exponential decays, pointing towards a first-order type process. A similar shape is found for the S_{bd} case after an initial faster decay that might be due to depletion of near-surface layers. The bulk diffusion limited case B_{bd} shows no clear behavior and thus seems to have a higher order dependence on concentration and time. As many experimental studies do not directly monitor the decay of bulk material, but rather loss of trace gas from the gas phase, we include the behavior of the effective reactive uptake coefficient $\gamma_{eff,X}$ for all limiting cases on a linear and logarithmic time scale in **(c)** and **(d)**. In addition to the eight regular limiting cases, we also display the traditional reacto-diffusive case, B^{rd}_{trad}, which shows a quadratic decay of N_Y as a function of time.

ACPD
13, 983–1044, 2013

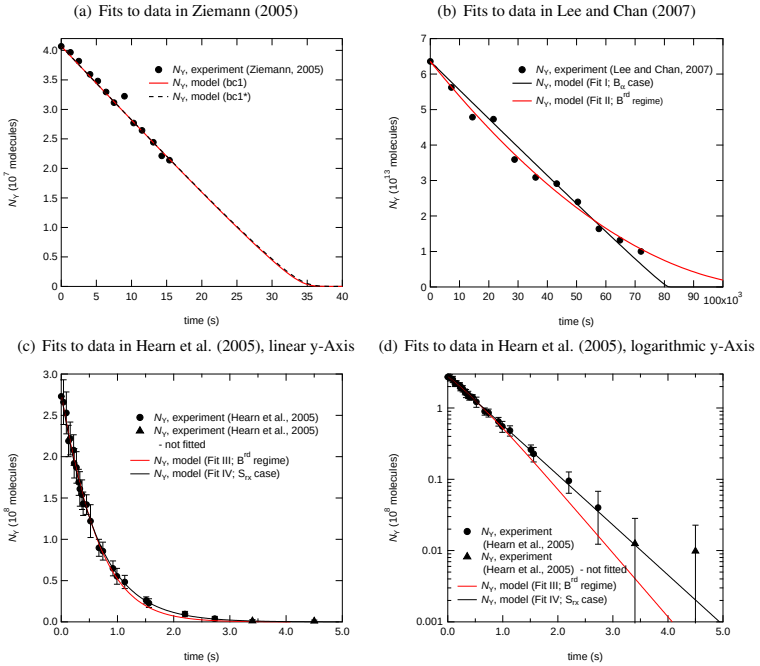

Fig. 6. Comparison of experimental and modeled data of various limiting cases, using time invariant kinetic parameters. In **(a)** the two parameter sets bc1 and bc1* lead to the same correlation with the experimental data and show the appropriate linear decay. In **(b)**, data from Lee and Chan (2007) show another mostly linear decay of bulk material. This can be realized with two KM-SUB parameter sets similar to bc1* showing B_α and B^{rd} behavior, respectively. In **(c)**, data from Hearn et al. (2005) show a non-linear decay that thus can not be described by accommodation-limited cases. The B^{rd} and S_{rx} fits shown are in excellent agreement with the experimental data. **(d)** reveals in a logarithmic representation that the quality of Fit III is lower after ~2 s and 85 % of the reaction. The last two points of this data set (black triangles) were excluded from the fit as their value is not significantly different from zero.

ACPD
13, 983–1044, 2013

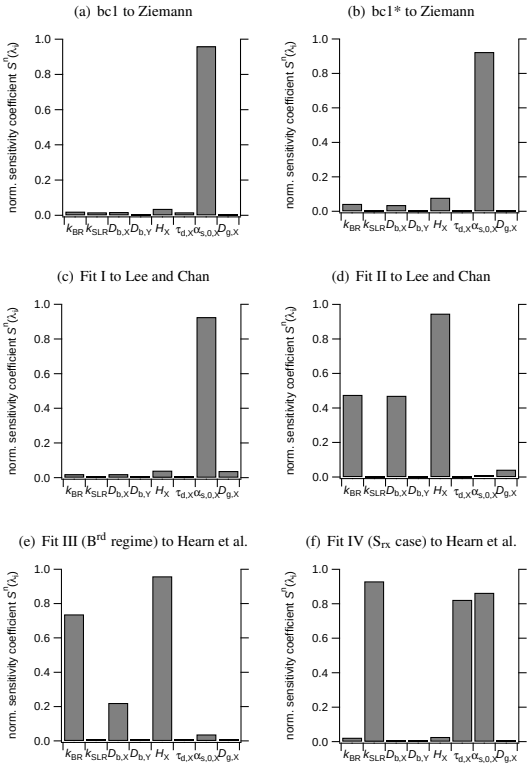

Fig. 7. Sensitivity profiles of parameter sets for a KM-SUB simulation of oleic acid – ozone. The parameter values used to generate these fits are shown in Table 6. Data sets are: **(a)** and **(b)**, Ziemann (2005); **(c)** and **(d)**, Lee and Chan (2007); **(e)** and **(f)**, Hearn et al. (2005). These sensitivity tests corroborate the limiting case and regime assignments made in this study, and indicate that the 9 : 1 criterion is sufficient to separate limiting case behaviors. The sensitivity coefficients were determined via Morris' Elementary Effects method for global sensitivity analysis (Morris, 1991) as recommended by Saltelli et al. (2008).

ACPD
13, 983–1044, 2013